Southeastern Geology: Volume 47, No. 2 May 2010

Editor in Chief: S. Duncan Heron, Jr.

Abstract

Academic journal published quarterly by the Department of Geology, Duke University.

SOUTHEASTERN GEOLOGY

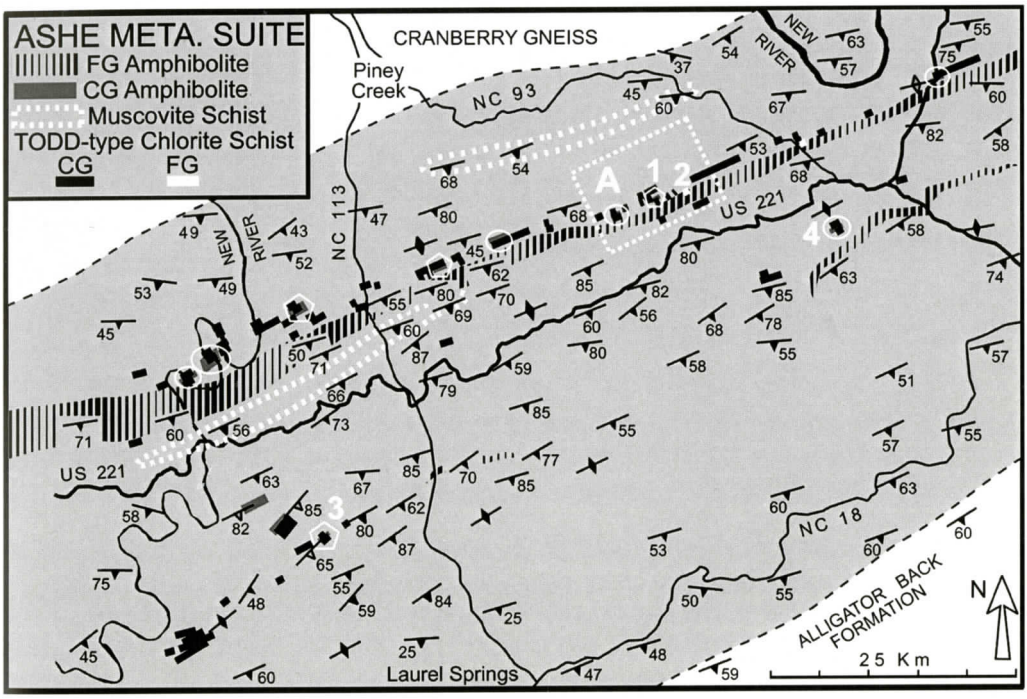

Vol. 47, No. 2 **May 2010**

SOUTHEASTERN GEOLOGY

PUBLISHED

at

DUKE UNIVERSITY

Duncan Heron

Editor-in-Chief

David M. Bush

Editor

This journal publishes the results of original research on all phases of geology, geophysics, geochemistry and environmental geology as related to the Southeast. Send manuscripts to **David Bush, Department of Geosciences, University of West Georgia, Carrollton, Georgia 30118, for Fed-X, etc. 1601 Maple St.,** Phone: 678-839-4057, Fax: 678-839-4071, Email: dbush@westga.edu. Please observe the following:

1) Type the manuscript with double space lines and submit in duplicate, or submit as an Acrobat file attached to an email.
2) Cite references and prepare bibliographic lists in accordance with the method found within the pages of this journal. Data citations examples can be found at http://www.geoinfo.org/TFGeosciData.htm
3) Submit line drawings and complex tables reduced to final publication size (no bigger than 8 x 5 3/8 inches).
4) Make certain that all photographs are sharp, clear, and of good contrast.
5) Stratigraphic terminology should abide by the North American Stratigraphic Code (American Association Petroleum Geologists Bulletin, v. 67, p. 841-875).
6) Email Acrobat (pdf) submissions are encouraged.

Subscriptions to *Southeastern Geology* for volume 47 are: individuals - $26.00 (paid by personal check); corporations and libraries - $40.00; foreign $55. Inquiries should be sent to: **SOUTHEASTERN GEOLOGY, DUKE UNIVERSITY, DIVISION OF EARTH & OCEAN SCIENCES, BOX 90233, DURHAM, NORTH CAROLINA 27708-0233**. Make checks payable to: *Southeastern Geology*.

Information about **SOUTHEASTERN GEOLOGY** is on the World Wide Web including a searchable author-title index 1958-2010 (Acrobat format). The URL for the Web site is: http://www.southeasterngeology.org

SOUTHEASTERN GEOLOGY is a peer review journal.

ISSN 0038-3678

SOUTHEASTERN GEOLOGY

Table of Contents

Volume 47, No. 2 May 2010

SOUTHEASTERN GEOLOGY
V. 47, No.2, May 2010, p. 61-84

ALTERED AMPHIBOLITE HYPOTHESIS FOR THE ORIGIN OF TODD-TYPE CHLORITE BODIES IN THE ASHE METAMORPHIC SUITE (AMS), NW NORTH CAROLINA

FRANK W. STAPOR, JR.

Dept. of Earth Sciences
Box 5062
Tennessee Tech University
Cookeville, TN 38505
fstapor@tntech.edu

SAMUEL E. SWANSON

Department of Geology
University of Georgia
Athens, GA 30602-2501

CHRIS FLEISHER

Department of Geology
University of Georgia
Athens, GA 30602-2501

ABSTRACT

Bodies of chlorite amphibole schist within the Late Proterozoic-Early Paleozoic Ashe Metamorphic Suite (AMS) in northwest North Carolina have been divided into Edmonds- and Todd-types based on modal mineralogy and bulk geochemistry (Scotford and Williams, 1983). Todd-type chlorites have a sheet-like geometry, meters- to several 10's of meters-thick and 10's of meters to several kms long and are concordant with the regional Ashe foliation. Where contact relationships can be determined, Todd-type coarse-grained schists (CGCS) are in sharp contact with coarse-grained amphibolites; Todd-type fine-grained schists (FGCS) are in sharp contact with fine-grained amphibolites and locally contain included decimeter-size, angular blocks of fine-grained amphibolites.

Chlorites from Todd-type and Edmonds-type rocks have significantly different (5% level) compositions. Using the method of Zane and Weiss (1998), which is specifically designed for microprobe analyses, all of these chlorites can be broadly classified as Mg-rich Type I.

Sampled Todd-type CGCS and their adjacent coarse-grained amphibolites have very similar amphibole mineralogies and paragenetic sequences. Both have relict magnesio-hornblende grains, rich in Fe/Ti-oxide inclusions, as the initial amphibole phase which is overgrown and largely replaced by Mg-rich actinolite (0.87±0.03 Mg/Mg+Fe). In some amphibolites the actinolite is overgrown by an inclusion-free magnesio-hornblende. Cummingtonite is the final amphibole phase in both of these lithologies; it replaces the actinolite and chlorite grains. Sampled Todd-type FGCS and their adjacent fine-grained amphibolites also have similar amphibole mineralogies and paragenetic sequences. Both consist of a variety of hornblendes (magnesio-hornblende, tschermakite, and pargasite) that are overgrown or replaced with cummingtonite. MgO-CaO-Al_2O_3 bulk compositions of the fine- and coarse-grained amphibolites are statistically identical at the 5% level. However, these amphibolites' bulk compositions are different from their associated chlorite amphibole schists.

These similarities in amphibole mineralogies and paragenetic sequences argue that the adjacent coarse- and fine-grained chlorite schist/amphibolite couplets experienced a similar metamorphic history. The presence of plagioclase in the amphibolite and early cummingtonite in the CGCS are probably related to subtle differences in pre-metamorphic protolith compositions. Todd-type amphibole chlorite schists are here interpreted to be metasomatically altered amphibolites, which originally were gabbros, and are not metasomatically altered dunites as suggested by Scotford and Williams (1983). Edmonds rocks are metamorphosed dunites. Athough this Todd-type chloritization event occurred throughout the AMS in northwestern North Carolina and southwestern Virginia, it was spatially limited by some other factor, as yet unknown, because only very restricted portions of the coarse- and fine-grained amphibolite protoliths were affected.

INTRODUCTION

The Ashe Metamorphic Suite (AMS) (Abbott and Raymond, 1984) of northwestern North Carolina consists of a heterogeneous assemblage of metamorphic rocks dominated by laminated, quartzo-feldspathic gneiss, fine- and coarse-grained amphibolite, and muscovite schist, plus dispersed masses of chlorite-rich schist and ultramafic rocks. Strictly speaking, the term ultramafic is reserved for igneous rocks with a high color index (little or no modal feldspar and/or quartz). The AMS was originally named the "Ashe Formation" by Rankin (1970). Abbott and Raymond (1984) renamed it the Ashe Metamorphic Suite in conformity with the North American Stratigraphic Code (NACSN, 1983) in recognition of its complex assemblage of metamorphic lithologies and multiple periods of metamorphism. A polymetamorphic history for the AMS was first described by Butler (1973).

Many workers in the southern Appalachians use the term ultramafic to describe rocks composed of amphibole, chlorite and talc believing the protoliths were igneous ultramafic rocks (e.g. Rankin *et al.*, 1972; Misra and Keller, 1978). Raymond and Warner (2001) discuss this issue and suggest using metaultramafic to emphasize the metamorphic character of these rocks.

The AMS of northwestern North Carolina and southwestern Virginia, where the Ashe Formation is placed in the Lynchburg Group (Henika,1997), contains bodies of metadunite and chlorite amphibole schists mapped as ultramafic rocks (Rankin *et al.*, 1972). Rankin, *et al.* (1972) showed the chlorite-rich bodies, on their 1:250,000 maps as small, lens-like masses within their Ashe "Formation". In eastern Ashe County, NC, and in all of Alleghany County, NC, they commonly mapped the chlorite-rich bodies adjacent to and on the northwest side of a prominent, fine-grained, amphibolite unit. Scotford and Williams (1983) divided these bodies of ultramafic rock in the AMS into Edmonds- and Todd-types based on modal mineralogy and bulk geochemistry. Mineral assemblages within individual bodies are variable, but most of the rocks are chlorite tremolite schists making the rocks metaultramafic rocks. Olivine-bearing rocks occur in both Todd and Edmonds-type bodies; but are more common in the Edmonds-type bodies (Scotford and Williams, 1983). Scotford and Williams (1983) proposed a similar (dunite) protolith for Edmonds and Todd-type bodies and interpreted differences in bulk compositions (and mineral assemblages) to reflect the degree of metasomatic alteration of the protolith.

Here we report on the detailed field relationships, mineral compositions, and whole-rock geochemistry of Todd-type chlorite amphibole schist bodies in Alleghany County, NC, and in adjacent parts of the counties of Ashe (NC) and Grayson (VA). The rarity of olivine (its lower Mg content) in the Todd-type rocks defines the difference between these rocks and Edmonds-type rocks. Todd-type bodies also have a much different spatial distribution, occurring as discontinuous sheet-like masses, most of which are arranged in linear chains along a single, 50-km long belt parallel to a prominent fine-grained amphibolite.

PREVIOUS WORK

The Ashe Formation (AMS) is dominated by thin layered, fine-grained, sulfide-bearing, biotite-muscovite gneiss with associated mica schist and amphibolite at its type locality in Ashe County, NC (Rankin 1970; *et al.*, 1973). As noted, Abbott and Raymond (1984) renamed the unit the Ashe Metamorphic Suite in recognition of the association of diverse metamorphic lithologies and in order to bring the name in compliance with the stratigraphic code (NACSN, 1983). Graywacke and shale are commonly considered to be the protoliths of the gneiss and mica schists, respectively and bulk compositions generally support this interpretation (Rankin *et al.*, 1973; Abbott and Raymond, 1984). Ashe gneisses to the south in Asheville, NC, have sandstone bulk compositions (Miller and Fryer, 1996), and similarly, the Ashe gneisses of the Gossan Lead District of Virginia have like compositions (Gair and Slack, 1984). Polymictic metaconglomerate, containing some granite clasts, was reported in basal Ashe gneiss by Rankin (1971). Whisonant and Tso (1992) report that metaconglomerate increases in abundance to the northeast, in Virginia. Basalts and gabbros have been interpreted as the protoliths for the interlayered fine- and coarse-grained amphibolites, respectively, by Rankin *et al.* (1973), Abbott and Raymond (1984), and Misra and Conte (1991). Chlorite schists and metadunite have both been considered to have ultramafic protoliths (Scotford and Williams, 1983; Abbott and Raymond, 1984; Raymond *et al.*, 2003).

Rankin *et al.* (1973) hypothesized that the Ashe "Formation" originally was a unit deposited on a rifted continental margin and had a nonconformable contact with the underlying Grenville-age Cranberry Gneiss. Wehr and Glover (1985) suggested a deep-water depositional environment for both the Ashe "Formation" and Lynchburg Group. The AMS is considered to be a subduction-related mélange by Raymond and coworkers (Abbott and Raymond, 1984; Raymond *et al.*, 1989; Raymond *et al.*, 2003) and Adams and coworkers (Willard and Adams, 1994; Adams *et al.*, 1995). Abbott and Raymond (1984) interpreted the Ashe/Cranberry contact to be a fault rather than a nonconformity. Misra and Conte (1991) interpreted the geochemistry of the Ashe amphibolites to indicate that the basalt protoliths of the Ashe fine-grained amphibolites were tholeiitic and generated at a spreading center, possibly a back-arc basin. They concur with Vincent (1983) that the Ashe amphibolites are chemically distinct from and unrelated to metabasalt intrusions within the adjacent, older Cranberry gneiss.

The AMS is the primary host for alpine-type ultramafic rocks in the central Blue Ridge. Misra and Keller (1978) summarized the petrology and occurrence of many Appalachian ultramafic rocks and concluded that the lenticular, dunite bodies of the Blue Ridge were tectonically emplaced as solid masses during the Taconic Orogeny. These bodies lack evidence of igneous intrusion and show up to five metamorphic overprints (Swanson, 1981; 2001; Abbott and Raymond, 1984; Raymond, 1995, p. 667 ff.; Raymond *et al.*, 2003). Swanson (2001) concluded that the ultramafic rocks of the Spruce Pine, NC, region should be considered metamorphic rocks and that the olivine compositions show systematic changes in relation to olivine abundance and coexisting mineral assemblages, a result which complicates the use of olivine composition as a protolith indicator. Warner and Hepler (2005) showed an increase in the iron content of olivine with increasing proportions of hydrous minerals present in metaultramafic rocks at Dark Ridge, NC.

Stose and Stose (1957) used the terms metadunite and metaperidotite in reference to rocks at Edmonds, NC near the Virginia border. Small-scale regional mapping of Rankin *et al.* (1972) of northwestern North Carolina shows a belt of ultramafic bodies lying northwest of a prominent fine-grained amphibolite; however, there are other occurrences outside of this belt. Abbott and Raymond (1984) suggested that this belt-like arrangement may be the result of faulting. Scotford and Williams (1983) made the first detailed examination of ultramafic rocks in the present study area of northwestern North Carolina and southwestern Virginia and sepa-

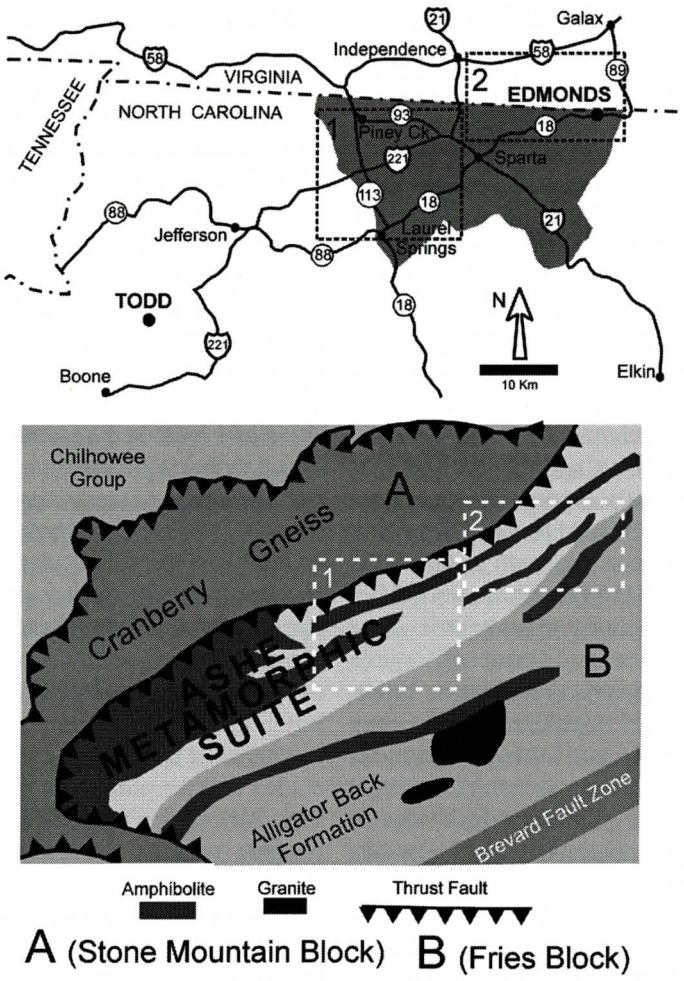

Figure 1. Location and general geology maps of the study area in northwestern North Carolina. Areas designated 1 and 2 are the locations of Figures 2 and 3. The names Todd and Edmonds are the type localities for the two kinds of coarse-grained, chlorite amphibole schist (CGCS) recognized by Scotford and Williams (1983). Alleghany Co., NC, is shown in gray; Ashe Co., NC, is located immediately west of Alleghany and Grayson Co., VA, immediately to the north.

rated them into the previously mentioned two groups, Edmonds- and Todd-types. Most of the described Blue Ridge ultramafic bodies are located tens to many tens of kilometers to the southwest of the study area.

The suggestion of a mélange origin for the AMS (Abbott and Raymond, 1984; Raymond *et al.*, 1989; Raymond *et al.*, 2003) has important implications for the determination of protoliths for the mafic and ultramafic rocks. Fragmentation and a lack of internal stratigraphy are two key elements in mélange units. Fragmentation and incorporation of blocks of mafic and ultramafic rocks within the AMS preceded the peak metamorphism and recrystallization as evidenced by the similar foliation attitudes and metamorphic grade between the blocks and enclosing mica schists and geneisses of the AMS. However, the minimum 125 kilometer-long, fine-grained, amphibolite present in this region is perhaps somewhat troublesome for the mélange model. Mafic rocks of the AMS have a range of compositions suggesting various tectonic settings (Hatcher *et al.*, 1984; Misra and

Figure 2. Typical exposure of Todd-type CGCS in the study area. The exposure extends all along the tree-line in this pasture. Strike measurements are reliable, but dip orientations are minimum estimates. The surrounding Ashe gneiss is mantled by soil.

Condie, 1991; Berger *et al*, 2001.; Ryan *et al.*, 2005) and this is consistent with the tectonic incorporation of blocks of mafic rocks from various tectonic settings within the mélange prior to accretion to North America. Ultramafic rock bodies within a mélange are also expected to be derived from a variety of crustal and subcrustal mantle settings with a variety of protoliths.

REGIONAL GEOLOGY

The study area is located in Alleghany County, NC, and the immediately adjacent parts of Ashe County, NC, and Grayson County, VA (Fig. 1). The AMS in this area is part of the Gossan Lead Block (thrust sheet) (Raymond, 1998; Raymond *et al.*, 2003; Hatcher *et al.*, 2006). Amphibolite facies metamorphism characterizes the AMS in this study area (with a biotite + garnet + kyanite + staurolite zone to the southwest and a biotite + staurolite + garnet zone to the northeast separated by a boundary located approximately along the Ashe/Alleghany county line (Rankin *et al.*, 1972; Abbott and Raymond,1984; 1997) (Fig. 1). AMS foliations define a NE/SW regional strike and dip southeast from 40 to 80+ degrees. Fine-grained amphibolites occur in continuous belts that extend many tens of kilometers across northwestern North Carolina and southeastern Virginia (Fig 1). Elongate belts of amphibolite are not representative of the more complex, polyphase folding revealed on a outcrop scale (Raymond *et al.*, 1989). Rankin, *et al.* (1972) showed the chlorite-rich bodies, on their 1:250,000 maps as small, lens-like masses within the Ashe Metamorphic Suite. In eastern Ashe County, NC, and in all of Alleghany County, NC, they commonly mapped the chlorite-rich bodies adjacent to and on the northwest side of a prominent, fine-grained, amphibolite unit.

DESCRIPTION OF TODD- AND EDMOND-TYPE METAULTRAMAFIC BODIES

Todd-type rocks are greenish-gray, chlorite amphibole schists. Chlorite and some elongate amphibole grains define a foliation that wraps around more rounded amphibole grains. The schists have two textures: 1) coarse-grained and 2) fine-grained. The coarse-grained chlorite amphibole schist (hereafter referred to as CGCS) commonly contains 5-10 mm vugs, partially filled with limonite, resulting from the weathering of a Fe-rich carbonate mineral. CGCS bodies outcrop as trains of resistant, meter-scale blocks projecting 1-3 meters above the Ashe regolith (Fig. 2). The fine-grained chlorite amphibole schist (hereafter referred to as FGCS) occurs immediately adjacent to or within fine-grained amphibolite. Foliations within the chlorite-rich rocks parallel foliation within the surrounding amphibolites and mica gneisses. The CGCS of this study corresponds to the Todd-type chlorite bodies of Scotford and Wil-

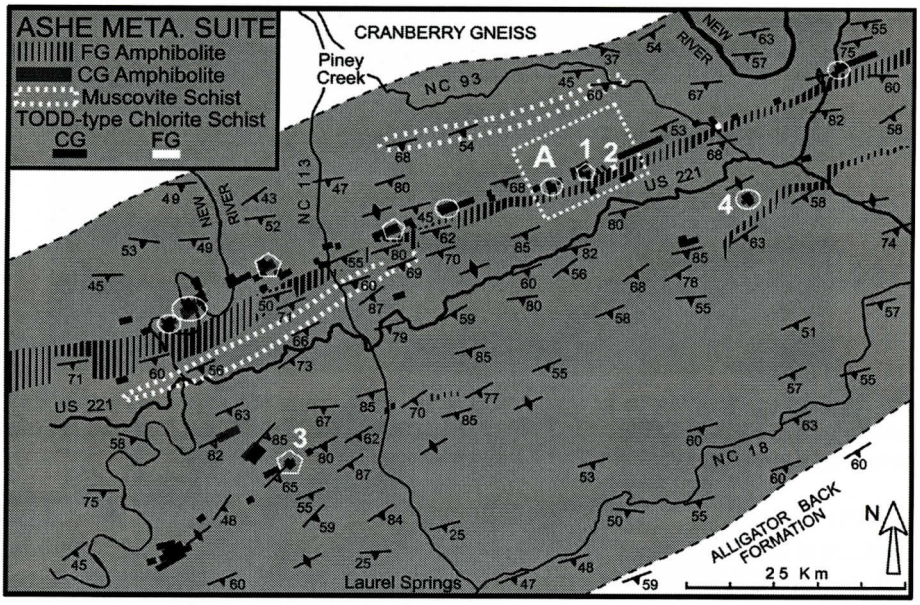

Figure 3. Geologic map showing AMS lithologies in area 1 (Fig. 1) the southwestern part of the study area. The four white pentagons locate where the actual contacts of Todd-type CGCS and adjacent Ashe lithologies can be observed; the six white ellipses locate where Todd-type CGCS and adjacent Ashe lithologies are between 0.25- and 1-meter apart. The majority of the Todd-type CGCS and the coarse-grained amphibolites are in a 3-kilometer wide belt immediately northwest of the northwestmost, prominent, fine-grained amphibolite within the Ashe Formation, however, there are numerous such chlorite bodies and coarse-grained amphibolites further to the southeast. The Todd-type FGCS are in contact with this prominent, fine-grained amphibolite. The white rectangle locates Figures 5-8. This diagram is taken in part from 7.5 Minute Quadrangle-scale mapping done by Stapor during the course of this study.

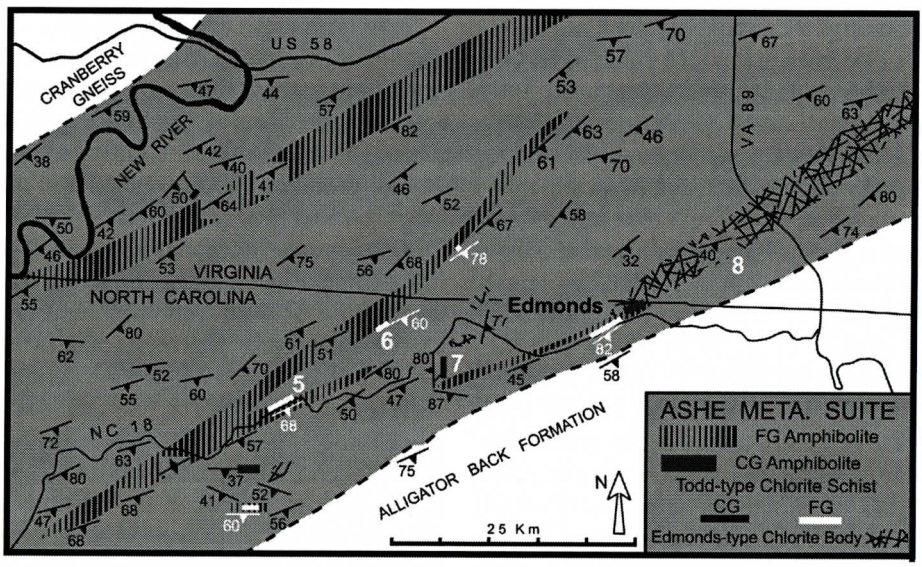

Figure 4. Geologic map showing AMS lithologies in the northeastern part of the study area, the rectangle labeled 2 in Fig. 1. There is only one Todd-type CGCS body in this portion of the study area. The Todd-type FGCS are in contact with fine-grained amphibolites. This diagram is taken in part from 7.5 Minute Quadrangle-scale mapping done by Stapor during the course of this study.

Table 1A. Bulk compositions (wt.% oxide) of representative coarse- and fine-grained chlorite schists and their respective adjacent coarse- and fine-grained amphibolites from the study area. The designated localities are shown on Figure 3. The designations (A)-(F) are for distinct samples shown in Figure 11. These analyses were made using the Inductively Coupled Plasma Emission Spectrophotometry (ICP) technique by Actlabs-Skyline of Tucson, AZ.

	Locality 1		Locality 3				
	CGCS	CGAM	CGCS (F)	CGCS (D)	CGAM (C)	CGAM (B)	CGAM (A)
SiO2	45.84	51.58	46.39	44.33	49.85	48.32	49.56
Al2O3	6.19	14.51	6.48	6.47	15.42	14.91	9.32
Fe2O3	13.85	9.41	12.97	12.86	8.69	8.49	10.85
MnO	0.194	0.149	0.209	0.192	0.14	0.156	0.237
MgO	26.69	8.43	20.81	22.48	9.56	11.93	16.31
CaO	0.26	10.41	8.07	6.28	12.68	12.52	12.46
Na2O	0.05	3.01	0.19	0.14	2.34	2.26	1.39
K2O	0.03	0.75	0.05	0.05	0.44	0.32	0.33
TiO2	0.647	1.002	0.388	0.536	0.748	0.827	0.553
P2O5	0.1	0.1	0.07	0.09	0.1	0.13	0.05
LOI	6.72	1.49	5.33	5.95	0.88	0.9	-0.07
Total	100.56	100.84	100.95	99.38	100.84	100.76	100.99

Table 1B. Bulk compositions (wt.% oxide) of representative coarse- and fine-grained chlorite schists and their respective adjacent coarse- and fine-grained amphibolites from the study area. The designated localities are shown on Figures 3 and 4. These analyses were made using the Inductively Coupled Plasma Emission Spectrophotometry (ICP) technique by Actlabs-Skyline of Tucson, AZ.

	Locality 2		Locality 4		Locality 5	
	FGCS	FGAM	CGCS	CGAM	FGCS	FGAM
SiO2	46.7	52.63	47.6	49.17	46.17	48.4
Al2O3	8.93	14.72	5.33	15.88	11.14	14.2
Fe2O3	12.42	14.16	11.71	4.8	12.42	17.39
MnO	0.226	0.188	0.219	0.125	0.191	0.263
MgO	18.57	5.14	22.16	8.31	16.01	6.53
CaO	7.81	7.79	8.71	14.76	9.38	8.93
Na2O	0.58	1.58	0.17	1.44	1.5	2.56
K2O	0.06	0.31	0.05	0.27	0.11	0.28
TiO2	0.717	1.806	0.539	0.571	0.127	1.265
P2O5	0.1	0.16	0.1	0.05	0.03	0.1
LOI	3.31	2.32	4.22	3.28	2.26	1.03
Total	99.42	100.81	100.8	98.66	99.33	100.93

liams (1983).

The Edmonds-type bodies contain dark to light-colored, chlorite, talc, amphibole schists with locally abundant relict olivine and magnetite porphyroblasts. They occur as isolated, lens-like masses, with long axes that range in size from 10's of meters to many 10's of kilometers that are orientated parallel to the NE-SW strike of the AMS regional foliation. The Edmonds body that "defines" this type is arguably the largest such altered ultramafic mass in the southern Appalachians, it extends some 60 kms

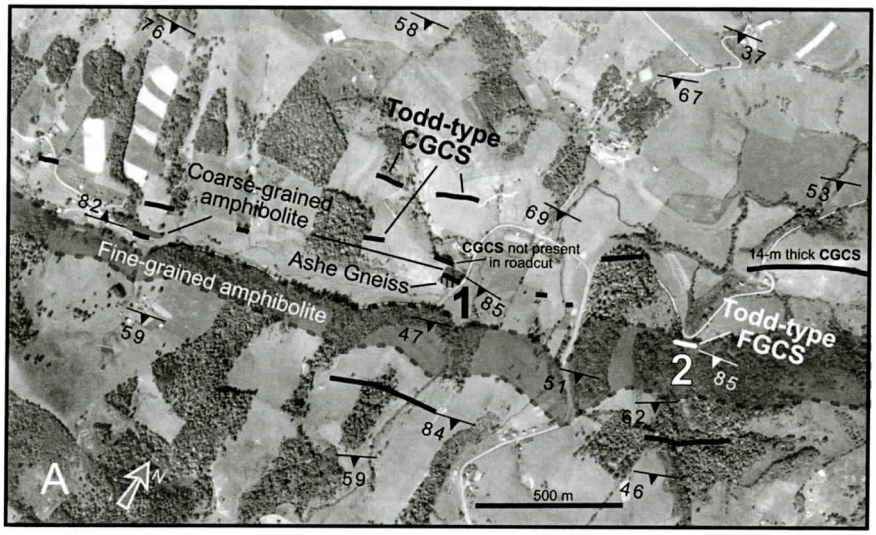

Figure 5. Geologic map of rectangle A (Fig. 3) on aerial photo base. The black number one locates the best road-cut exposure in the study area of a Todd-type CGCS in contact with adjacent Ashe lithologies. In addition, at locality one the northern CGCS does not extend out into the road-cut and terminates within 15 meters along strike. At white number two a Todd-type FGCS occurs within albeit at the northern margin of the fine-grained amphibolite. The CGCS bodies occur primarily along the northwestern margin of the fine-grained amphibolite, however, there are two CGCS bodies located to the southeast.

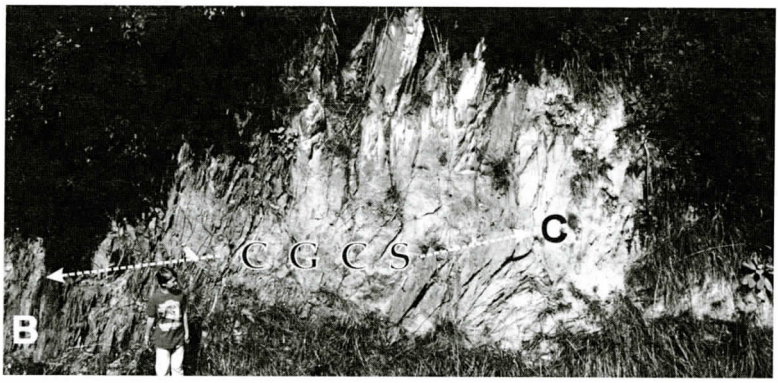

Figure 6. Road-cut exposure of Todd-type CGCS in direct contact with Ashe laminated gneiss (B) and coarse-grained amphibolite (C), locality 1 in Figure 5. The distance across the CGCS is 5 meters.

northeast into Virginia from its named locality at Edmonds on the NC/VA state line; 25 kms of this body are shown in Fig. 4.

LOCAL FIELD RELATIONSHIPS

Coarse-Grained Schists (CGCS)

The typical Todd-type CGCS exposure in the study area is a two to three meter wide, line of meter-scale blocks that extends for many tens to many hundreds of meters (Fig. 2). The contacts can only be seen in rare natural exposures and equally rare road-cuts. Where contacts are observable, the chlorite body has either 1) sharp boundaries with gneiss on one side and a coarse-grained amphibolite on the other, or 2) sharp boundaries with coarse-grained amphibo-

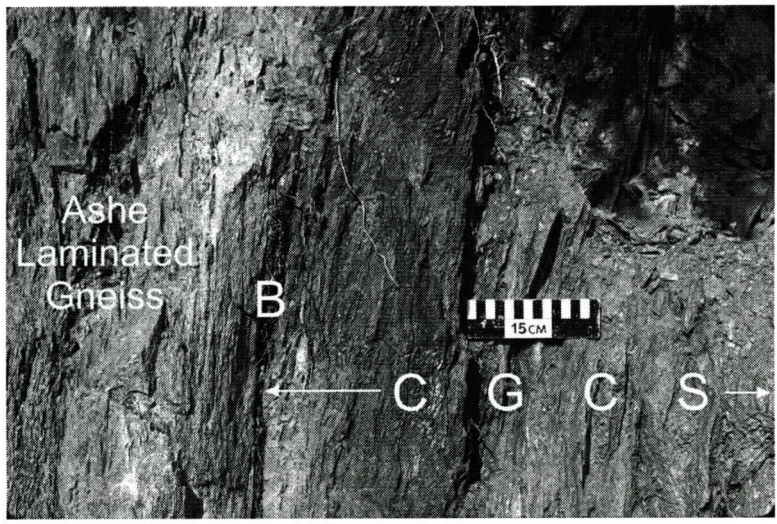

Figure 7. Detail view of CGCS contact with Ashe laminated gneiss at position B in Figure 6. The white letter B is at the contact.

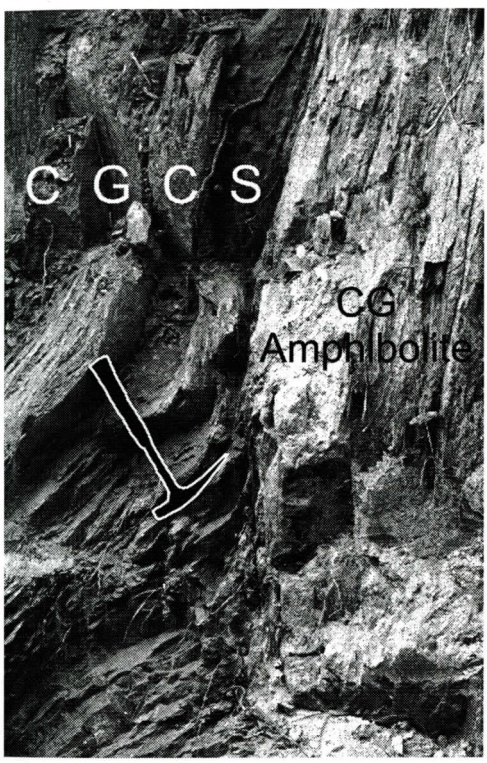

Figure 8. Detail view of CGCS contact with coarse-grained amphibolite at position C in Figure 6.

lites on both sides. In addition, commonly the CGCS bodies terminate abruptly along strike within a distance of several meters, whereas the adjacent coarse-grained amphibolite continues further along strike. The results of more detailed mapping (Figs. 3 and 4), conducted primarily in winter months, show the general relations of the Todd- and Edmond-type chlorite schist bodies to the enclosing rocks of the AMS. The majority of the Todd-type CGCS bodies in the study area occur in a 3-kilometer wide belt on the northwestern flank of a prominent, fine-grained amphibolite within the AMS. This is also the location of most of the newly discovered coarse-grained amphibolites (Fig. 3). Numerous Todd-type CGCS bodies also occur southwest of this prominent fine-grained amphibolite. An excellent exposure of a Todd-type CGCS and the adjacent AMS is present near Piney Creek, NC (locality 1 of Figures 3 and 5). In this area, there are 13 separate CGCS bodies in a belt within 400 meters of the northwestern boundary of the prominent fine-grained amphibolite and two more within 200 meters southeast of it. The CGCS exposed in the roadcut at locality 1 is approximately 5 meters wide, perpendicular to foliation (Fig. 6). The southeastern contact with the AMS gneiss is sharp (Fig. 7) and the 25 or so cms of chlorite schist immediately adjacent to the contact has a crinkled fabric. The northwestern contact with a coarse-grained amphibolite is sharp (Fig. 8). There is one additional exposure of coarse-

Figure 9. Detail of fine-grained amphibolite block (white X) within a Todd-type FGCS, locality 6 in Figure 4. The amphibolite block foliation is parallel to that of the FGCS and the immediately adjacent (out of view) fine-grained amphibolite.

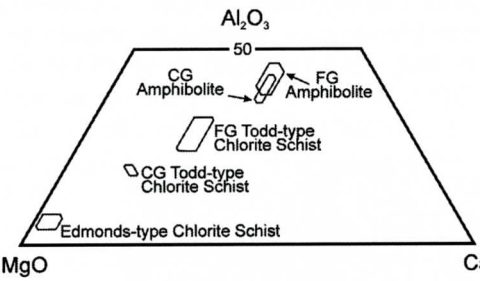

Figure 10. Bulk compositions of the various chlorite bodies and amphibolites from the AMS in the northwest North Carolina study area. The 95% confidence interval polygons about the means of the various rock types are shown in this diagram. Edmonds-type and Todd-type schist data are from Scotford and Williams (1983) and this study. The coarse-grained amphibolite data are from this study. The fine-grained amphibolite data are from this study with the addition of two samples from Conte (1986) and Misra and Conte (1991). The two amphibolites are statistically identical based on the overlap of their confidence polygons. The Todd-type FGCS are more similar to their immediately adjacent fine-grained amphibolites than are the Todd-type CGCS with their immediately adjacent coarse-grained amphibolites.

grained amphibolite adjacent to, but not in direct contact with, a CGCS near the southwestern end of the CGCS belt (Fig. 5). Todd-type CGCS bodies generally parallel the regional Ashe foliation.

Fine-Grained Schists (FGCS)

The Todd-type FGCSs are in contact with fine-grained amphibolite (Figs. 3 and 4).

Chlorite schist bodies are associated with the contacts of fine-grained amphibolite (localities 2 and 6, Figs. 3, 4 and 5). A small inclusion of fine-grained amphibolite in chlorite schist (locality 7, Fig. 4) is shown on Figure 9 and illustrates the close association of the Todd-type FGCS and fine-grained amphibolite. Foliations of the FGCS and the fine-grained amphibolite are generally parallel.

BULK COMPOSITIONS OF CHLORITE BODIES AND AMPHIBOLITES

Bulk chemical analyses of coarse and fine-grained chlorite amphibole schist and adjacent amphibolites were made at Actlabs-Skyline of Tucson, AZ, using the Inductively Coupled Plasma Emission Spectrophotometry (ICP) technique. Representative analyses are given in Tables 1A and 1B. Scotford and Williams (1983) also did bulk chemical analyses on coarse and fine-grained chlorite amphibole

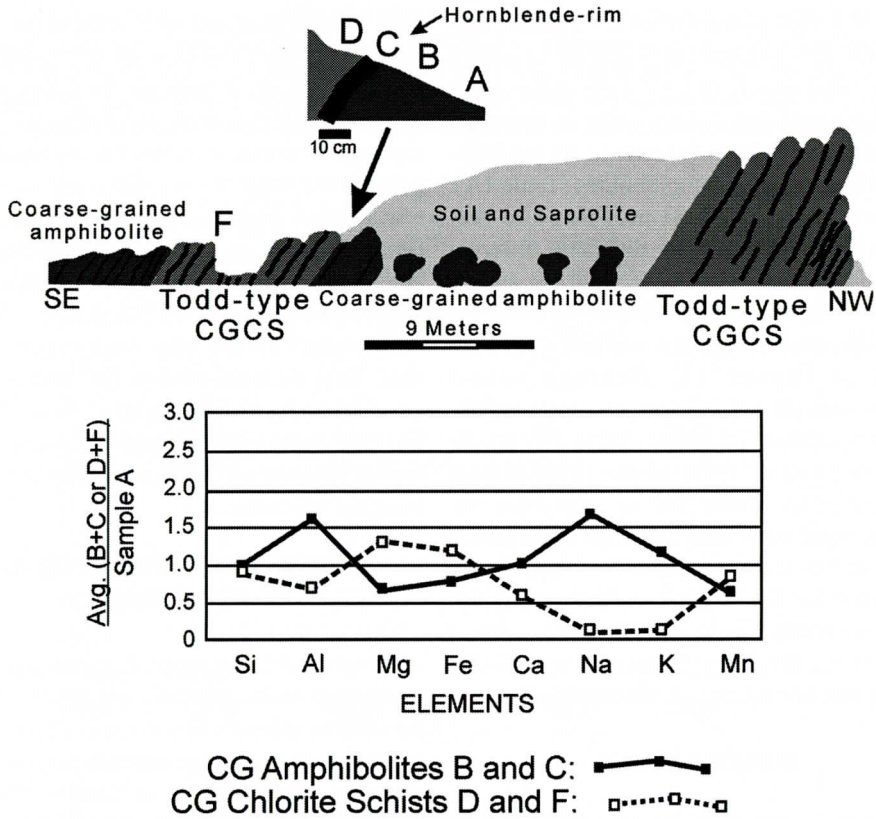

Figure 11. Outcrop sketch of creek bank at Locality 3, Fig. 3. There are two separate Todd-type CGCS either in contact with or immediately adjacent to coarse-grained amphibolite. The insert describes one of the exposed contacts and locates samples, A-D, F taken across this contact. A normalized profile using coarse-grained amphibolite A as the standard is shown below. The two amphibolite samples B and C have essentially identical proportions relative to the standard amphibolite A; the two coarse-grained chlorite schist samples D and F likewise have essentially identical proportions relative to the standard amphibolite A. See text for details.

schist, but did not report values for silica.

A MgO-CaO-Al2O3 ternary diagram (Fig. 10) shows the data from the present study along with the Scotford and Williams data expressed as 95% confidence interval polygons about the means of the various rock types. Edmonds- and Todd-type chlorite schists have significantly different bulk compositions, the Todd-type contain more calcium and aluminum and less magnesium than the Edmonds-type rocks. Coarse and fine-grained amphibolites are statistically identical in bulk composition and their 95% confidence interval polygons overlap (Fig. 10). Coarse and fine-grained chlorite amphibole schists, however, have different bulk compositions. The fine-grained schists are higher in Al than the coarse-grained schists (Fig. 10).

Bulk compositional analyses of several samples along a traverse (locality 3 of Fig. 3) across a typical Todd-type, coarse-grained chlorite schist (CGCS) and its immediately adjacent coarse-grained amphibolite (CGAM) are reported in Table 1A. Samples A, B, and C are coarse-grained amphibolites and D and F are coarse-grained chlorite schists (CGCS). Amphibolites are slightly higher in SiO_2 (48 to 50 weight percent) than the chlorite schists (44 to 46 weight percent SiO_2). The amphibolites contain 9-16 weight percent MgO, 9-15 weight percent Al_2O_3, 12-13 weight percent CaO and 8-11 weight percent Fe_2O_3. The chlorite-rich rocks are lower in Al_2O_3 (6-7 weight percent) and

CaO (6-8 weight percent) than the adjacent amphibolites, but are higher in MgO (20-22 weight percent) and Fe_2O_3 (12-13 weight percent). Amphibolites B and C are similar in composition, but amphibolite A is lower in Al and higher in Ca than the other amphibolites (Table 1A). Chlorite schists (samples D and F) are also similar in composition, but are distinctly different from adjacent amphibolites (samples B and C, Table 1A, Fig. 11). Compositional variation between adjacent amphibolites and schists is illustrated in Figure 11. Average schist compositions (D and F, Table 1A) and amphibolite compositions (B and C, Table 1A) are divided by compositions of the most distant amphibolite (A, Table 1A) to emphasize the compositional contrasts. Silica contents are all similar at this scale, but there is an antisympathetic variation the in other elements. Amphibolites are enriched in Al, Ca, Na, and K relative to the schists (Fig. 11). Schists are enriched in Fe, Mg, and Mn relative to the amphibolites.

MINERALOGY

Chlorite + amphibole + minor CrFeTi oxide (consisting of magnetite, chromian magnetite, or ilmenite) is the characteristic mineral assemblage of the Todd-type, coarse grained, chlorite schists (CGCS). Scotford and Williams (1983) report these rocks also contain minor amounts of dolomite, olivine and talc. Trace amounts of augite with coronas of amphibole were noted in several of the samples. Small amounts of carbonate (magnesite) were noted in some of our samples, but we did not observe olivine or talc. Modal abundances of the various phases were not determined in this study, but the high abundance of chlorite + amphibole (> 80 modal percent) indicated by Scotford and Williams (1983) was confirmed by our observations. Amphibolites associated with the Todd-type chlorite bodies, CGCS and FGCS, contain abundant amphibole, plagioclase, and quartz; lesser amounts of chlorite and zoisite/clinozoisite and trace amounts of FeTi oxides.

Electron microprobe analyses were made of selected minerals from CGCS and FGCS Todd-type schists and from their adjacent amphibolites. These analyses were done at the University of Georgia's Department of Geology using a JEOL JXA-8600 Superprobe running Geller Microanalytical Laboratory's dQANT32 stage and spectrometer automation. Analyses were performed with an accelerating voltage of 15KV, 15nA beam current, approximately 1 um beam diameter, and 10 second counting times. Natural and synthetic mineral standards were used, and analyses were calculated using J. T. Armstrong's (1988) phi-rho-z matrix correction. Total Fe is reported as FeO and oxygen is calculated by stoichiometry. Backscattered electron photomicrographs were acquired using Geller Microanalytical Laboratory's dPICT32 imaging software.

Amphibole Petrography and Mineralogy

Amphibole is the most abundant phase in the Todd-type rocks, typically accounting for over 50 volume percent of the rocks (Scotford and Williams, 1983). Calcic amphiboles analyzed in this study show a range of compositions from magnesio-hornblende to tschermakite to tremolite/actinolite. Low-Ca cummingtonite was also identified as a late-stage overgrowth on calcic amphibole. Complex corona textures of amphiboles on amphiboles are common in the chlorite-rich rocks.

The most common amphibole in the CSCG Todd-type bodies and the adjacent coarse-grained amphibolites is Mg-rich actinolite (Tables 2A, 2B, and 3), according to the AMPH-IMA04 classification program (Mogessie *et al.*, 2004, which uses microprobe compositions as inputs) and the classification scheme of Leake *et al.* (1997). This Mg-rich actinolite is immediately below the arbitrary divide between tremolite and actinolite on the Leake *et al.* (1997) classification diagram and is probably analogous to the tremolite reported by Scotford and Williams (1983). Cores of magnesio-hornblende are overgrown by the common Mg-rich actinolite (Figs. 12, 13) in the CGCS from localities 3 and 4 (Figs. 3 and 11). The adjacent coarse-grained amphibolites at localities 3 and 4 also contain these relict magnesio-hornblende

Table 2A. Compositions (wt.% oxide) and numbers of atoms of representative amphiboles from Todd-type coarse-grained chlorite schists (CGCS) and adjacent coarse-grained amphibolites (CGAM). Localities 3 and 4 are found on Figure 3. Atomic numbers were determined using the AMPH-IMA04 classification program (Mogessie *et al.*, 2004) which uses microprobe compositions as inputs. FeO*=total Fe as FeO. Mg-hbd1=magnesio-hornblende. Mg-act2=Magnesium-rich actinolite.

	Locality 3 CGCS Remnant Core Fe/Ti blebs	Locality 3 CGCS Overgrowth	Locality 3 CGAM Dominant	Locality 4 CGCS Remnant Core Fe/Ti blebs
	Mg-hbd1	Mg-act2	Mg-act2	Mg-hbd1
SiO2	47.85	56.41	56.47	47.32
TiO2	0.29	0.05		0.41
Al2O3	8.38	1.41	0.68	8.00
MgO	15.98	20.15	21.02	16.64
FeO*	11.58	7.73	0.17	10.21
CaO	12.4	12.49	6.9	11.51
MnO	0.23	0.27	12.45	0.20
Na2O	1.48	0.27	0.16	1.56
K2O	0.36	0.03	0.04	0.47
Cr2O3	0.04			0.42
total	98.59	98.81	97.89	96.74
O	23	23	23	23
Si	6.811	7.799	7.85	6.822
Ti	0.031	0.005	0.004	0.044
Al	1.406	0.23	0.111	1.359
Mg	3.391	4.153	4.356	3.576
Fe2+	0.832	0.735	0.665	0.656
Fe3+	0.547	0.159	0.137	0.575
Ca	1.891	1.85	1.854	1.778
Mn	0.028	0.032	0.02	0.024
Na	0.408	0.072	0.043	0.436
K	0.065	0.005	0.007	0.086
Cr	0.004			0.048
total	15.414	15.04	15.047	15.404

grains overgrown by the common Mg-rich actinolite (Fig. 14). These magnesio-hornblendes are aluminous and are compositionally distinct from the other amphiboles (Fig. 15, Tables 2A and 2B). At locality 3 (Figs. 3 and 11) the relict magnesio-hornblende replaces augite in the amphibolite at the contact of the CGCS (Figs. 11 and 16). These inclusion-rich, relict magnesio-hornblende grains are very rare in both the CGCS and their adjacent coarse-grained amphibolites.

Todd-type FGCS occurs within and in contact with FGAM. At localities 2 and 5 (Figs. 3 and 4), the amphiboles in the amphibolites are predominately tschermakite. In the adjacent chlorite schists, however, the amphibole is predominately magnesio-hornblende and a late stage cummingtonite (Fig.17, Table 3). The chlorite schist at locality 5 also contains tschermakite, which frequently overgrows a magne-

Table 2B. Compositions (wt.% oxide) and numbers of atoms of representative amphiboles from Todd-type coarse-grained chlorite schists (CGCS) and adjacent coarse-grained amphibolites (CGAM). Locality 4 is found on Figure 3. Atomic numbers were determined using the AMPH-IMA04 classification program (Mogessie *et al.*, 2004) which uses microprobe compositions as inputs. FeO*=total Fe as FeO. Mg-hbd1=magnesio-hornblende. Mg-act2=Magnesium-rich actinolite.

	Locality 4 CGCS Overgrowth	Locality 4 CGAM Remnant Core Fe/Ti blebs	Locality 4 CGAM Overgrowth	Locality 4 CGAM Dominant
	Mg-act2	Mg-hbd1	Mg-act2	Mg-act2
SiO2	56.38	48.89	56.69	57.34
TiO2		0.43		
Al2O3	1.08	7.16	0.52	0.31
MgO	21.62	17.27	21.20	21.49
FeO*	5.99	9.95	6.80	5.52
CaO	12.76	12.20	12.93	13.28
MnO	0.25	0.22	0.34	0.16
Na2O	0.30	1.62	0.15	0.08
K2O		0.23		0.04
Cr2O3		0.34		
total	98.38	98.31	98.63	98.23
O	23	23	23	23
Si	7.775	6.931	7.82	7.911
Ti		0.046		
Al	0.176	1.196	0.085	0.05
Mg	4.445	3.65	4.36	4.42
Fe2+	0.499	0.695	0.552	0.537
Fe3+	0.192	0.485	0.233	0.1
Ca	1.885	1.853	1.911	1.963
Mn	0.029	0.026	0.04	0.019
Na	0.08	0.445	0.04	0.021
K		0.042		0.007
Cr		0.038		
total	15.081	15.407	15.041	15.028

sio-hornblende core (Fig. 18). The FGCS have an amphibole mineralogy different from their adjacent amphibolites, locally less aluminous and generally more Mg- and Fe-rich, whereas the CGCS and their adjacent coarse-grained amphibolites have essentially identical amphibole mineralogies.

CHLORITE MINERALOGY

Chlorite occurs in the interstitial areas between grains of amphibole in all of the chlorite schists, but is a rare phase in the amphibolites. Foliation in the chlorite schists is defined by alignment of chlorite flakes around the coarser-grained amphibole crystals. Chlorite contains between 18 and 22 weight percent Al_2O_3 and is low in Cr (0.0 to 0.3 weight percent Cr_2O_3).

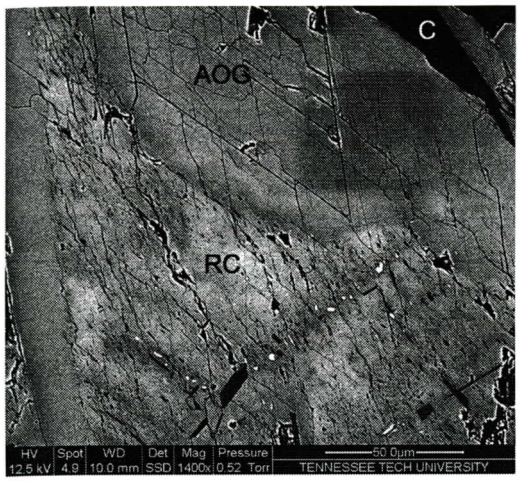

Figure 12. BSI (back scatter image) of relict magnesio-hornblende (RC) core with Mg-rich antinolite (AOG) overgrowth, Todd-type CGCS, locality 4 (Fig. 3). The relict core and overgrowth are in optical continuity. Note the bright Fe/Ti blebs within the relict core. The dark material (C) is Mg-rich, Type I chlorite (classification of Zane and Weiss, 1998).

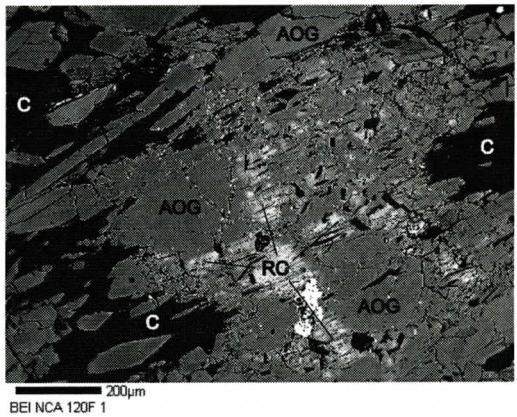

Figure 13. BSI of relict magnesio-hornblende (RC) core with Mg-rich actinolite (AOG) overgrowth, Todd-type CGCS, locality 3 (Fig. 3). The relict cores and overgrowths are in optical continuity. The dark material (C) is Mg-rich, Type I chlorite (classification of Zane and Weiss, 1998).

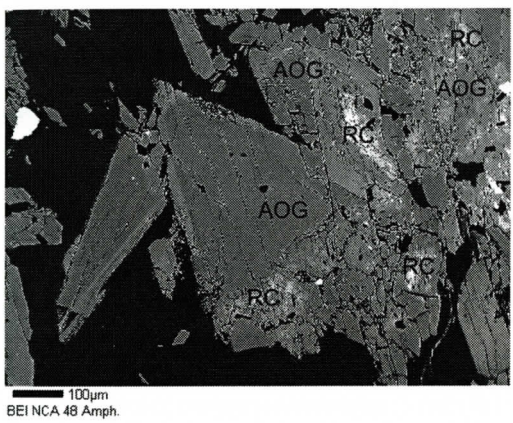

Figure 14. BSI of relict magnesio-hornblende (RC) core with Mg-rich antinolite (AOG) overgrowth, coarse-grained amphibolite, locality 4 (Fig. 3). The relict cores and overgrowths are in optical continuity. Compositional zoning is present in many of the Mg-actinolite overgrowths. The dark material is feldspar.

Using the Zane and Weiss (1998) method of broadly (?) classifying chlorites based on microprobe analyses, both Edmonds- and Todd-type chlorites are Mg-rich Type I (Fig. 19 and Table 4). However, the four analyzed chlorite sets (Fig. 19) are all significantly different at the 5% level. Although the 95% confidence polygons are rather small, the Todd-type CGCS chlorites and one of the Edmonds-type chlorites (locality 8) have the largest amount of variability.

DISCUSSION

Detailed field mapping shows a variety of contact relationships and host rocks for Todd-type chlorite bodies. 1) CGCS are immediately adjacent to CGAM on one side and either another such amphibolite or the common AMS gneiss on the other. 2) CGCS are immediately adjacent to fine-grained amphibolites. CGCS also occur throughout the AMS, not in association with any amphibolite. FGCS occurs only with FGAM.

Sampled Todd-type CGCS and their adjacent coarse-grained amphibolites have very similar amphibole mineralogies and paragenetic sequences at localities 3 and 4 (Figs. 3 and 12). Both have relict magnesio-hornblende grains,

Table 3. Compositions (wt.% oxide) and numbers of atoms of representative amphiboles from Todd-type fine-grained chlorite schists (FGCS) and adjacent fine-grained amphibolites (FGAM). Locality 2 is found on Figure 3; Locality 5 is found on Figure 4. Atomic numbers were determined using the AMPH-IMA04 classification program (Mogessie *et al.*, 2004) which uses microprobe compositions as inputs. FeO*=total Fe as FeO. Mg-hbd1=magnesio-hornblende. Tsch2=Tschermakite. Cumm3=Cummingtonite.

	Locality 2 FGCS Dominant	Locality 2 FGAM Dominant	Locality 5 FGCS Remnant Core no Fe/Ti blebs	Locality 5 FGCS Overgrowth	Locality 5 FGCS Late-stage	Locality 5 FGAM Dominant
	Mg-hbd1	Tsch2	Mg-hbd1	Tsch2	Cumm3	Tsch2
SiO2	52.33	43.31	50.03	43.69	55.72	42.56
TiO2	0.18	0.42	0.11	0.12		0.64
Al2O3	6.32	15.38	8.04	14.60	0.55	13.25
MgO	17.49	9.02	16.57	13.30	20.71	9.32
FeO*	0.19	16.39	9.34	12.01	18.07	17.68
CaO	7.80	12.14	11.59	11.07	0.71	11.73
MnO	12.48	0.28	0.16	0.12	0.75	0.39
Na2O	0.63	0.40	0.11	0.13	0.07	0.27
K2O	0.07	1.40	1.10	1.86	0.02	1.63
total	97.50	98.74	97.05	96.90	96.60	97.47
O	23	23	23	23	23	23
Si	7.365	6.338	7.107	6.309	7.954	6.34
Ti	0.019	0.046	0.012	0.013		0.072
Al	1.048	2.653	1.346	2.485	0.093	2.326
Mg	3.669	1.968	3.509	2.863	4.407	2.07
Fe2+	0.767	1.797	0.751	0.82	1.803	1.739
Fe3+	0.151	0.209	0.359	0.63	0.354	0.464
Ca	1.882	1.903	1.764	1.713	0.109	1.872
Mn	0.023	0.035	0.019	0.015	0.091	0.049
Na	0.172	0.397	0.303	0.521	0.019	0.471
K	0.013	0.075	0.02	0.024	0.004	0.051
total	15.109	15.421	15.421	15.19	14.834	15.454

rich in Fe/Ti-oxide inclusions, as the initial amphibole phase, which is overgrown and largely replaced by Mg-rich actinolite. Cummingtonite is the final amphibole phase in both of these lithologies; as it replaces the actinolite. At locality 3 (Fig. 11), amphibolite sample C contains relict cores of augite surrounded by magnesio-hornblende with FeTi oxide inclusions (Fig. 16). A rim of inclusion-free magnesio-hornblende encloses the augite/inclusion-rich grains (Fig. 16). This inclusion-free magnesio-hornblende is seen to overgrow actinolite in some amphibolegrains in sample C. The inclusion-rich grains of magnesio-hornblende appear to form by the replacement of clinopyroxene.

The masses of FGCS are found within FGAM and blocks of FGAM are enclosed in FGCS (Fig. 9). Sampled Todd-type FGCS contain inclusion-free magnesio-hornblende, locally overgrown with tschermakite. The common amphibole present in the adjacent fine-grained amphibolite is tschermakite (Fig. 18). The lack of FeTi inclusions in the magnesio-hornblende

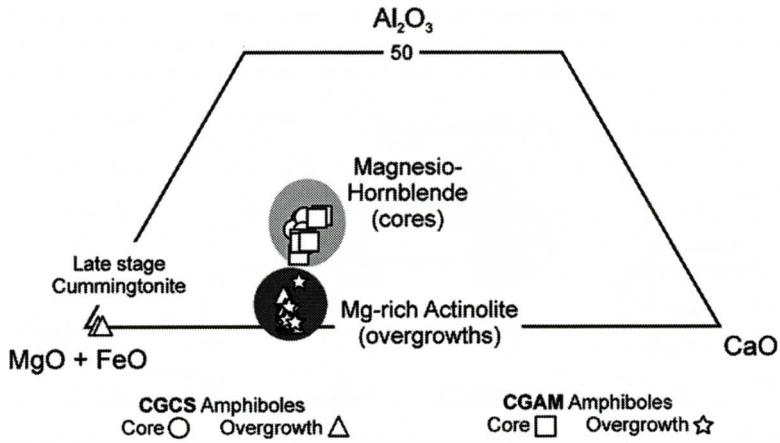

Figure 15. Composition and classification of amphiboles in Todd-type coarse-grained chlorite schist (CGCS) and adjacent coarse-grained amphibolite (CGAM) at localities 3 and 4 (Fig. 4). The AMPH-IMA04 program (Mogessie *et al.*, 2004) was employed to determine Mg/Mg+Fe and number of Si Atoms used to name or classify the amphiboles according to the scheme of Leake *et al.* (1997). The open circles and squares represent magnesio-hornblende grains that contain abundant Fe/Ti blebs; the open triangles and stars represent mg-rich actinolite overgrowths on magnesio-hornblende cores and/or the predominantly occurring amphibole.

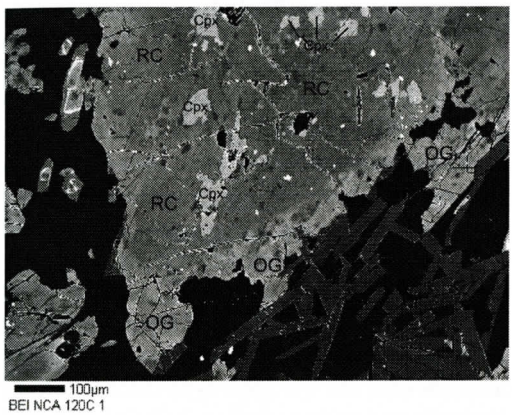

Figure 16. BSI of clino-pyroxene (Cpx) with overgrowths of magnesio-hornblende with Fe/Ti blebs (RC) followed by a second, more Fe-rich magnesio-hornblende (OG), sample C (CGAM) at locality 3 (Figs. 3 and 11). The two magnesio-hornblendes are in optical continuity.

may indicate a lack of clinopyroxene in the protolith of the FGCS. Bulk compositions of the FGCS are intermediate between CGCS and the amphibolites (Fig. 11). The elevated Al content of the FGCS relative to the CGCS is reflected in the more Al-rich tschermakitic amphibole. FGCS in the study area probably resulted from local mixing and/or metasomatic alteration between amphibolite and amphibole chlorite schist.

We did not find any olivine in our samples of Todd-type CGCS. This contrasts with the report of Scotford and Williams (1983), in which minor amounts of forsterite with compositions of 88 and 90 mol% Fo were recorded for Edmonds- and Todd-type bodies, respectively. They interpreted these olivines to be relict and a direct indicator of ultramafic protoliths. We preformed microprobe analyses on olivine in rocks from the type localities of the Todd-type and Edmonds-type chlorite bodies. Compositions of olivine from the large body at Edmonds, NC is Mg-rich, 92 $\pm$ 0.4 mol% Fo (five analyses), similar to olivine from other metadunites in the Blue Ridge (Swanson, 2001; Warner, 2001, Warner and Helper, 2005). Olivine in the body at Todd, NC, outside of our study area, is more Fe-rich, 72 $\pm$ 0.6 mol% Fo (6 analyses), similar to olivine from chlorite amphibole olivine schists in the Piedmont of SC (Warner and Griffin, 1989). Differences in olivine compositions are related to differences in bulk composition between the Edmonds and Todd rocks.

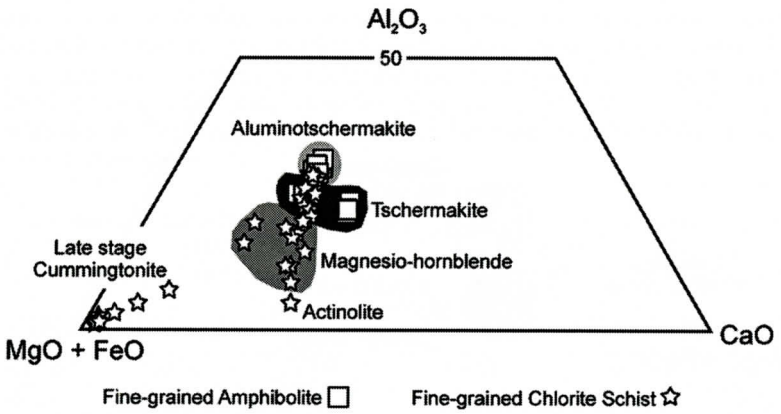

Figure 17. Composition and classification of amphiboles in Todd-type fine-grained chlorite schist (FGCS) and adjacent fine-grained amphibolite (FGAM) at localities 2 and 5 (Figs. 3 and 4). See caption Figure 15 for details. The tschermakite within the FGCS occurs primarily as overgrowths on magnesio-hornblende grains.

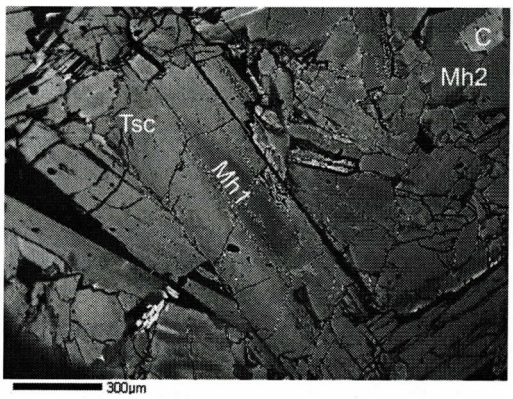

Figure 18. BSI of fine-grained chlorite schist (FGCS) at locality 5 (Fig. 4) The black grains are chlorite, all of the remaining grains are amphiboles. Mh is magnesio-hornblende and Tsc is tscher-makite. The large grain in the center magnesio-hornblende core (Mh1) that is overgrown with tschermakite (Tsc). In the upper right-hand corner there is a magnesio-hornblende grain (Mh2) being replaced with cummingtonite (

INTERPRETATION

Compositions of the Todd-type amphibole chlorite schists are intermediate between the metaultramafic rocks of the Edmonds-type bodies and the amphibolites (Fig. 10). Various workers have inferred an igneous protolith (tholeiite basalt flows and shallow intrusions) for these amphibolites (Bryant and Reed, 1970; Bottino, 1971; Rankin *et al.*, 1973; Abbott and Raymond, 1984; Conte, 1986; Misra and Conte, 1991). We concur with the dunite and peridoitite protolith interpretation for the Edmonds-type bodies of Stose and Stose (1957) and Scotford and Williams (1983). The position of the Todd-type amphibole chlorite schists' analyses intermediate between the Edmonds-type and the amphibolites (Fig. 10) suggests two general possibilities: 1) a protolith intermediate between basic and ultrabasic composition or 2) the metasomatic alteration of either a basic or ultrabasic protolith. The field association of the amphibolites and the Todd-type chlorite schists strongly suggests a genetic relationship and thus the above two considerations are restricted to variations in and/or modifications to the respective, adjacent amphibolites.

Analyses of the amphibole chlorite schists from Scotford and Williams (1983) and this study, the Edmonds-type chlorite schists from Scotford and Williams (1983), and the amphibolite analyses from this study, Conte (1986), and Misra and Conte (1991) are shown on a Al_2O_3 – CaO variation diagram (Fig. 20). Fields for cumulate gabbro and ultramafic (pyroxenites and peridotites) rocks identified by Lippard, *et al.*, (1986) from the basal magmatic part of the Oman ophiolite sequence are also

Table 4. Compositions (wt.% oxide) and numbers of atoms of representative chlorites for the study area. Localities 2-4 are found on Figure 3; Localities 5-8 are found on Figure 4. All chlorites are Mg-rich, Type I of Zane and Weiss (1998). FeO*=total Fe as FeO.

	Todd-type FGCS Locality 2	Todd-type CGCS Locality 3 (F)	Todd-type CGCS Locality 4	Todd-type FGCS Locality 5	Edmonds Locality 7	Edmonds Locality 8
	chlorite	chlorite	chlorite	chlorite	chlorite	chlorite
SiO2	27.39	28.54	28.4	27.61	27.25	30.25
Al2O3	22.02	19.09	19.68	21.92	21.94	18.97
MgO	23.9	25.01	24.5	24.13	24.92	32.27
FeO*	12.49	14.92	14.99	13.18	12.49	5.51
total	85.8	87.56	87.57	86.84	86.6	87.00
O	28	28	28	28	28	28
Si	5.49	5.68	5.65	5.48	5.42	5.77
Al	5.20	4.48	4.62	5.13	5.14	4.27
Mg	7.14	7.42	7.27	7.14	7.38	9.18
Fe	2.09	2.49	2.50	2.19	2.08	0.88
total	19.91	20.07	20.04	19.95	20.01	20.09

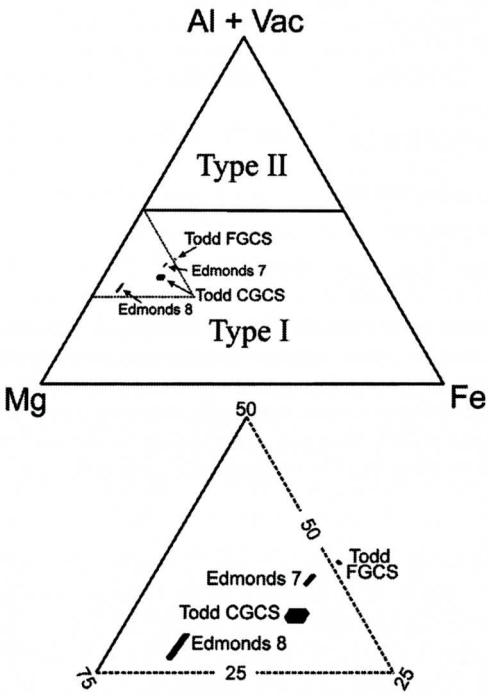

Figure 19. This ternary diagram shows chlorite microprobe compositions using the method of Zane and Weiss (1998). The 95% CI polygons about the mean of each data set are plotted in this diagram. All of these data sets are statistically different. Both the Edmonds- and Todd-type chlorites in this study are Mg-rich Type I.

shown on Figure 20. The associated coarse- and fine-grained amphibolites plot either within or immediately adjacent to the gabbro field (Fig. 20), a result in agreement with protolith interpretations of previous workers. All but two of the Edmonds-type chlorite schists plot either within or adjacent to the peridotite field (Fig. 20), again in agreement with protolith interpretations of previous workers.

Four of the six Todd-type, FGCS samples plot either within or immediately adjacent to the gabbro field, a situation that strongly suggests that the associated fine-grained amphibolites were their protoliths (Fig. 20). The two FGCS samples that plot well outside of the gabbro field are from localities 2 (Fig. 3) and 6 (Fig. 4). Both of these FGCS bodies are "sandwiched" between fine-grained amphibolites and Locality 6 contains recognizable blocks of fine-grained amphibolite that have the same structural orientation as the adjacent fine-grained amphibolites (Fig. 9). These field relationships make a compelling argument that the adjacent fine-grained amphibolites were indeed the protoliths of the FGCS at Localities 2 and 6.

One of the CGCS samples plots adjacent to the gabbro field and 7 or 8 plot within or immediately adjacent to the pyroxenite field; howev-

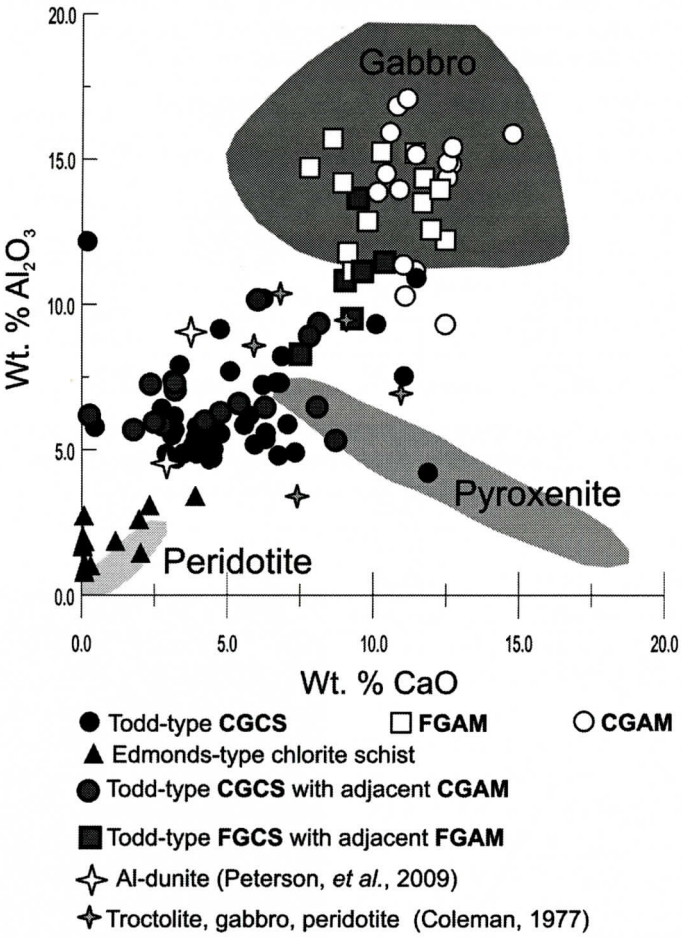

Figure 20. Variation diagram for samples of Edmonds-type chlorite schist, Todd-type chlorite amphibole schists, and fine- and coarse-grained amphibolites. Edmonds-type and Todd-type schist data are from Scotford and Williams (1983) and this study. The coarse-grained amphibolite data are from this study. The fine-grained amphibolite data are from this study with the addition of two samples from Conte (1986) and Misra and Conte (1991). Compositional fields for peridotite (dunite and harzburgite), pyroxenite, and gabbro are from the Oman ophiolite (Lippard, *et al.*, 1986).

er, the vast majority of CGCS samples plot somewhere intermediate between the gabbro, periodotite, and pyroxenite fields (Fig. 20). In Locality 3 (Figs. 3 and 11) one CGCS body is "sandwiched" between coarse-grained amphibolites; in all other CGCS localities where contacts could be observed, at least one contact is with a coarse-grained amphibolite. These field relationships coupled with the nearly identical amphibole paragenesis in both the CGCS and adjacent coarse-grained amphibolite make a very strong argument for a coarse-grained amphibolite protolith. A possible geochemical objection to this interpretation is the obvious reduction in Al-content in the CGCS. Al is widely supposed to be of such limited mobility, given its reported low solubility in supercritical fluids (Frantz *et al.*, 1981), that it is commonly used as a comparative standard to identify compositional changes, i.e. Ferry (1983). However, Chinner (1961), Foster (1981), Yardley (1977), Bucher-Nurminen (1982), Watkins (1983) and Kerrick (1988) suggest that Al can be relatively mobile, at least under conditions of prograde,

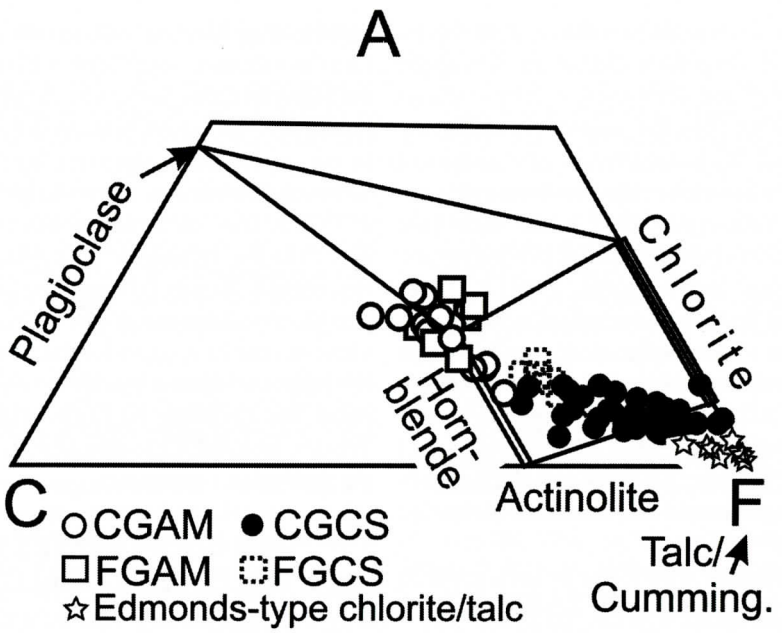

Figure 21. ACF diagram illustrating metamorphic mineral assemblages for amphibolites (CGAM, FGAM) and chlorite amphibole schist (CGCS, FGCS, Edmonds-type) from this study area. Differences in bulk compositions account for the presence (or absence) of plagioclase in these rocks. See text for details.

dehydration metamorphism. The compositional traverse shown in Fig. 11 can be qualitatively interpreted to indicate that during the rehydration of the part of the original coarse-grained amphibolite that now is a CGCS, Al, Ca, Na, and K were removed to the adjacent amphibolite and the adjacent amphibolite lost Mg and Fe to the now CGCS.

The alternate protolith interpretation for these CGCS samples is that they probably had other mafic and/or ultramafic (?) protoliths, such as the troctolites and peridotites of Coleman (1977), the gray stars in Fig. 20, or the Al-rich dunites of Peterson, *et al.* (2009), the white stars in Fig. 20. It may well be problematic that these different protoliths would have produced amphibole paragenetic sequences identical to those of their adjacent gabbros, now represented by the coarse-grained amphibolites. Mineral assemblages in metamorphic rocks are related to bulk rock compositions (along with other intensive variables like pressure, temperature, etc.). Compositions of the Todd-type amphibole-chlorite schists plot in the ultrabasic range on ACF diagrams (Fig. 21) and the amphibolites plot in the basic range. These differences in bulk composition control the presence of plagioclase in the amphibolites and the absence of plagioclase in the amphibole chlorite schists. More subtle variations in mineralogy, such as the differences in chlorite compositions in different rocks (Fig. 21) or the presence of tschermakitic amphibole in FGCS (Fig. 19), are also explained by differences in bulk rock compositions. Similarities and differences in mineralogy are related to variations in bulk composition. Cummingtonite is seen as a stable phase with calcic amphibole and chlorite in the chlorite amphibole schists (Fig. 21). The calcic amphibole/chlorite tie line screens the amphibolites from the cummingtonite. However, cummingtonite does occur in amphibolites as a late-stage overgrowth on calcic amphibole in amphibolites that do not contain chlorite.

CONCLUSIONS

Scotford and Williams (1983) defined the Todd-type CGCS bodies as tremolite chlorite schists with minor amounts of dolomite, oliv-

ine, and talc derived from a dunite protolith by metasomatic alteration. Our study found the mineralogy of the amphibole chlorite schists more complex than the model presented by Scotford and Williams (1983). The dominant amphibole is Mg-rich actinolite. No olivine occurs in the Todd-type CGCS in our study area (we did confirm the presence of olivine reported by Scotford and Williams (1983) in Todd-type rocks at Todd, NC, outside of our study area). The late-stage amphibole in the Todd-type rocks is cummingtonite rather than anthophyllite. We concur with the multi-stage recrystallization model presented by Scotford and Williams (1983), but we favor protoliths of gabbro that experienced metasomatic alteration during chloritization.

In all instances where one or both contacts between amphibole chlorite schists and adjacent rocks have been observed in this study, one of the adjacent rocks is an amphibolite, either fine- or coarse-grained. This close association of amphibolites and amphibole chlorite schists strongly suggests a relation between the two rock types. However, detailed geologic mapping shows that only portions of these amphibolites have been chloritized, suggesting that additional, and as yet unknown, factors are significant to the spatial distribution of the chloritization. Current mineralogy of these chlorite schists is the product of regional, retrograde metamorphism. Differences in mineral assemblages are related to differences in bulk rock composition; differences that were present prior to metamorphism. Protolith compositions appear to be gabbros similar to rocks found in ophiolites. The association of amphibole chlorite schists with amphibolites and metadunites discussed in this paper is found in other parts of the Blue Ridge (Raymond *et al.*, 1989; Swanson, 2001, *et al.*, 2005). Future workers should be careful to include these chlorite schists in their attempts to reconstruct petrotectonic assemblages of mafic and ultramafic rocks in the Appalachian Orogen.

ACKNOWLEDGEMENTS

The senior author wishes to acknowledge the assistance of Wayne Hawkins, Material Science Lab Coordinator, Tenn. Tech. University Center for Manufacturing Research, in the operation of the SEM. The results presented here are based in part upon work supported by the National Science Foundation under Grant No. DMR-0115961. The senior author has received support from the Tennessee Technological University Faculty Research Fund. The late Raymond and Shirley Simmons of Piney Creek, NC, provided extensive support for the field work done by the senior author. An earlier version of this paper was reviewed by Loren Raymond, Rich Warner, and Jeff Chaumba and we thank them for their useful comments.

UTM COORDINATES FOR SELECTED LOCALITIES

These UTM coordinates position the respective locality to within a 10-m square. All coordinates use the 1927 North American Datum and are within UTM Zone 17S.

Locality (Figs. 3, 4)	UTM Easting	UTM Northing
1	0480110	4041920
2	0480850	4042180
3	0472590	4034070
4	0484150	4041250
5	0496850	4043750
6	0499050	4045600
7	0496800	4042100
8	0500490	4044660

REFERENCES CITED

Abbott, R. N. and Raymond, L. A., 1984, The Ashe Metamorphic Suite, northwest North Carolina: metamorphism and observations on geologic history: American Journal of Science, v. 284, p. 350-375.

Armstrong, J.T., 1988, Quantitative analysis of silicate and oxide materials: comparison of Monte Carlo, ZAF, and phi (rho Z) procedures, *in* D.E. Newbury, ed., Microbeam Analysis, p 239-246.

Bryant, B. and Reed, J. C., Jr., 1970, Geology of the Grandfather Mountain Window and vicinity, North Carolina and Tennessee: U. S. Geological Survey Professional Paper 615, 195 p.

Bottino, M. L., 1971, Rb, Sr, and Sr isotope measurements of amphibolites from the Ashe Formation, North Caro-

lina (abs.): Geological Society of America Abstracts with Programs, v. 3, p. 297.

Bucher-Nurminen, K. 1982, On the mechanism of contact aureole formation in dolomitic country rock by the Adamello intrusion (northern Italy): American Mineralogist, v. 67, p. 1101-1117.

Butler, J. R., 1973, Paleozoic deformation and metamorphism in part of the Blue Ridge thrust sheet, North Carolina: American Journal of Science, v. 273-A, p. 72-88.

Chinner, G. A., 1961, The origin of sillimanite in Glen Clova, Angus: Journal of Petrology, v. 2, p. 312-323.

Coleman, R. G., 1977, Ophiolites: Springer-Verlag, New York.

Conte, J. A., 1986, Geochemistry and tectonic significance of amphibolites within the Precambrian Ashe Formation, northwestern North Carolina (MS thesis): Knoxville, TN. University of Tennessee, 122 p.

Ferry, J. M., 1983, Mineral reactions and element migration during metamorphism of calcareous sediments from the Vassalboro Formation, south-central Maine: American Mineralogist, v. 68, p. 334-354.

Foster, C. T., Jr., 1981, A thermodynamic model of mineral segregations in the lower sillimanite zone near Rangely, Maine: American Mineralogist, v. 66, p. 260-277.

Frantz, J. D., Popp, R. K., and Boctor, N. Z., 1981, Mineral-solution equilibria—V. Solubilities of rock forming minerals in supercritical fluids: Geochim et Cosmochim Acta, v. 45, p. 69-77.

Gair, J. E. and Slack, J. F., 1984, Deformation, geochemistry and origin of massive sulfide deposits, Gossan lead district, Virginia: Economic Geology, v. 79, p. 1483-1520.

Henika, William S., 1997, Geologic map of the Roanoke 30x60 minute quadrangle: Virginia Division of Mineral Resources, Report No. 148.

Kerrick, D. M., 1988, Al2SiO5-bearing segregations in the Lepontine Alps, Switzerland: Aluminum mobility in metapelites: Geology, v. 16, p. 636-640.

Leake, B. E., *et al.*, 1997, Nomenclature of amphiboles: Report of the Subcommittee on Amphiboles of the International Mineralogical Commission on New Minerals and Mineral Names: Min. Mag., Vol.61, p. 295-321.

Lippard, S.J., Shelton, A.W., and Gass, I.G., 1986, The ophiolite of northern Oman: Geological Society of London, Memoir, 11, 178 pp.

Miller, Jr., J. W. and Fryer, K. H., 1996, Geology of the Ashe Metamorphic Suite in the Beaucatcher Mountain road cut, Asheville, North Carolina: Southeastern Geology, v. 36, No. 3, p. 133-152.

Misra, K. and Keller, F. B., 1978, Ultramafic bodies in the southern Appalachians: a review: American Journal of Science, v. 278, p. 398-418.

Misra, K. and McSween, H. Y., Jr., 1984, Mafic rocks of the southern Appalachians: a review: American Journal of Science, v. 284, p. 294-318.

Misra, K. and Conte, J. A., 1991, Amphibolites of the Ashe and Alligator Back Formations, North Carolina:samples of Late Proterozoic-early Paleozoic oceanic crust: Bull. GSA, vol.103, p.737-750.

Mogessie, A., Ettinger, K., and Leake, B. E., 2004, AMPH-IMA04: a revised Hypercard program to determine the name of an amphibole from chemical analyses according to the 2004 International Mineralogical Association scheme: Min. Mag., Vol.68 (5), p. 825-830.

NACSN (North American Commission on Stratigraphic Nomenclature), 1983, North American Stratigraphic Code: American Association Petroleum Geologists Bulletin, v. 67, no. 5, p. 841-875.

Peterson, V., Ryan, J. G., Becker, A., Cochrane, D., Collins, J., Frey, B., Gaskin, P., Kates, K., Lee, A., Lindenberg, M. Lizee, T., Lucan, S., Manooch, S., McCoy A., Meyers, S., Morman, S. B., O'Leary, J., Olesky, M., Palmer, J., Pauley, T., Rahl, J., Simons, K., Slusser, T., Stonesifer, K., Thomas, C., and Thornberry, T., 2009, Petrogenesis and structure of the Buck Creek mafic-ultramafic suite, Southern Appalachians; constraints on ophiolite evolution and emplacement in collisional orogens: Bull. GSA, vol. 121, no. 3-4, p. 615-629.

Rankin, D. W., 1970, Stratigraphy and structure of Precambrian rocks in northwestern North Carolina, *in* Fisher, G. W., *et al.*, eds., Studies of Appalachian geology: central and southern: Interscience, New York, p. 227-245.

Rankin, D. W., 1971, Guide to the geology of the Blue Ridge in southwestern Virginia and adjacent North Carolina, *in* Guidebook to Appalachian tectonics and sulphide mineralization in southwestern Virginia: Virginia Polytech. Inst. and State Univ. Dept. of Geological Sciences Guidebook 5, p. 39-85.

Rankin, D. W., Espenshade, G. H., and Neuman, R. B.,1972, Geologic map of the west half of the Winston-Salem Quadrangle, North Carolina, Virginia, and Tennessee: USGS Miscellaneous Geologic Investigations, Map I-709-A.

Rankin, D. W., Espenshade, G. H., and Shaw, K. W., 1973, Stratigraphy and structure of the metamorphic belt in northwestern North Carolina and southwestern Virginia: a study from the Blue Ridge across the Brevard fault zone to the Sauratown mountains anticlinorium: American Journal of Science, v. 273-A, p. 1-40.

Raymond. L. A., Yurkovick, S. P., and McKinney, M., 1989, Block-in-matrix structures in the North Carolina Blue Ridge belt and their significance for the tectonic history of the southern Appalachian Orogen, *in* Horton, Jr., J. W. and Rast, N., eds, Melanges and Olistostromes of the U.S. Appalachians: Geological Society of America Special Paper 228, p. 195-215.

Scotford, D. M. and Williams, J. R., 1983, Petrology and geochemistry of metamorphosed ultramafic bodies in a portion of the Blue Ridge of North Carolina and Virginia: American Mineralogist, vol. 68, p.78-94.

Swanson, S. E., 2001, Ultramafic rocks of the Spruce Pine area, western North Carolina: a sensitive guide to fluid migration and metamorphism: Southeastern Geology, v. 40, no. 3, p. 163-182.

Vincent, H. B., 1983, Metamorphosed mafic dikes within the Cranberry Gneiss and their relation to amphibolites

of the Ashe Formation: North Carolina-Tennessee Blue Ridge (abs): Geological Society of America Abstracts with Program, v. 15, p. 51.

Watkins, K. P., 1983, Petrogenesis of albite porphyroblast schist: Geological Society of London Journal, v. 140, p. 601-618.

Wehr, R., and Gover, L., 1985, Stratigraphy and tectonics of the Virginia-North Carolina Bulue Ridge: Evolution of a Late Proterozoic hinge zone: Geological Society of American Bulletin, c. 96, p. 285-295.

Whisonant, R. C., and Tso, J. L., 1992, Stratigraphy and structure of the lower Ashe Formation (upper Precambrian) along the Fries Fault in southwestern Virginia: *in* Dennison, J. M. and Steward, K. G. (ed.), Geologic Field Guides to North Carolina and Vicinity, Southeastern Section, Geological Society of America, Univ. of North Carolina at Chapel Hill, Geologic Guidebook No. 1, p. 15-28.

Willard, R. A., and Adams, M. G., 1994, Newly discovered eclogite in the southern Appalachian orogen, northwestern North Carolina: Earth and Planetary Science Letters, v. 123, p. 61-70.

Yardley, B. W. D., 1977, The nature and significance of the mechanism of sillimante growth in the Connemara Schist, Ireland: Contributions to Mineralogy and Petrology, v. 65, p. 53-58.

Zane, A. and Weiss, Z., 1998, A procedure for classifying rock-forming chlorites based on microprobe data: Rend. Fis. Acc. Lincei, s.9, vol.9, p. 51-56.

SOUTHEASTERN GEOLOGY
V. 47, No.2, May 2010, p. 85-94

PERIGLACIAL FEATURES AND LANDFORMS OF THE DELMARVA PENINSULA

RUSSELL L. LOSCO

Lanchester Soil Consultants, Inc.
311 East Avondale Road
West Grove, PA, USA, 19390
Soildude@comcast.net

WILLIAM STEPHENS

Stephens Environmental Consulting, Inc.
P.O. Box 485
North East, MD, USA, 21901-0485
BStephens@stephensenv.com

MARTIN F. HELMKE

West Chester University
Department of Geology and Astronomy
207 Merion Science Center
West Chester, PA, USA, 19393
mhelmke@wcupa.edu

ABSTRACT

This study documents a paleosol impacted by periglacial features at a site on the Delmarva Peninsula of Southern Delaware. This paleosol is characterized by increased stiffness/density, change in matrix color, evidence of induration and cementation, relict fluvial versus aeolian sedimentary structures, secondary structures associated with permafrost or deep seasonal frost, and fossil roots and animal burrows. Partially-lignitized roots, root channels, animal burrows and secondary sedimentary structures associated with subaerial exposure and soil-forming processes truncate abruptly at the contact with the overlying massive, loose, aeolian sand. We hypothesize that this paleosol developed within fluvial beds of the Beaverdam Formation during a lengthy period of subaerial exposure. Several layers of parent material of different origins were noted: a) structureless clays, b) structureless aeolian sands, c) fluvial, normal-graded, cross-stratified, and laminated sands with gravel lag beds, and d) indurated, sandy clays interpreted to be a paleosol. Sufficient definition of the surface of this paleosol was obtained to reconstruct the paleotopography of the site, which is distinctly different from the current topography. We interpret this buried surface as a former land surface of early Pleistocene to late Pliocene age.

INTRODUCTION

Recent investigations have documented the presence of periglacial features on the East Coast of the United States farther south than previously thought. The objective of this study was to investigate landforms and subsurface features on the Delmarva Peninsula to determine if they support the presence of a periglacial paleoenvironment as far south as Southern Delaware. Although late Wisconsinan glaciers in Pennsylvania were considered to be separated from evergreen woodlands by no more than 100 km of tundra, recent data indicate that within the coastal plain of New Jersey and Delaware, sandy, well-drained, poorly-vegetated soils may have allowed tundra conditions to extend farther south than formerly thought. French and Demitroff (2001) state that the closed depressions commonly found on the Coastal Plain (sometimes referred to as "Carolina" basins) are considered to be deflation hol-

lows or blowouts formed by strong katabiatic winds originating from the glaciers to the north. These aeolian activities appear to be a significant force in the formation of the landscape. Sand wedges or sand-wedge relicts are described as examples of deep frost action. Cryoturbated soils and polygonal patterned ground are also noted as evidence of periglacial conditions.

Andres & Howard (1998) report wedge casts in the Scotts Corner Formation at the Pollack Farm site in Delaware. They interpret the wedge casts as fossil frost wedges formed in seasonally frozen ground based upon downward warping of adjacent beds.

Investigations of sites in the New Jersey coastal plain indicate that late Pleistocene permafrost extended as far south as 39° north latitude. Wedge casts, referred to as ground wedges, found in the area are interpreted as seasonal frost cracks infilled with loose aeolian frosted sands. Optically-stimulated-luminescence (OSL) dating of the infilled material indicates that the sands accumulated during two separate periods, one during the late Illinoian to early Wisconsinan glaciation (55-66 ka) and another during the late Wisconsinan glaciation (15-22 ka). Based upon the thermal contraction cracking in fine and coarse-grained sands, French et al. (2003) postulated that maximum mean annual air temperatures of <-4 and <-8 °C were common. Dislocation of near-surface ironstone deposits suggests that permafrost in this area reached thicknesses of 10-15 m (French et al., 2003).

Wedges filled with aeolian sand have been documented at two locations in New Castle County, Delaware at approximately 39° 44' and 39° 25' north latitude within the Columbia Formation. The Columbia Formation is composed of fluvial sands that accumulated approximately 400 ka with a surface discontinuity that is capped by loess that accumulated approximately 10 to 13 ka. Pollen assemblages indicate that the Columbia Formation accumulated during a transitional period from a cold, glacial stage to a warmer, inter-glacial period. The wedges found are consistently below the loess cap and therefore pre-date the last glacial maximum and

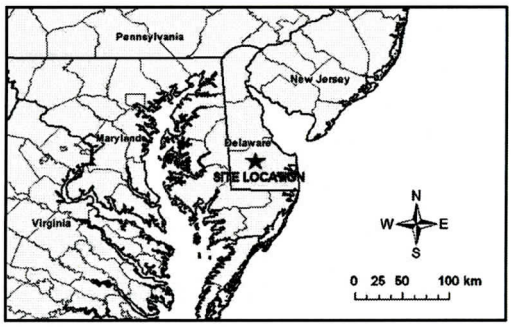

Figure 1. Site Location. The site is located on the Delmarva Peninsula, in the Coastal Plain Physiographic Province of the Mid-Atlantic Region in Sussex County Delaware at approximately 38° 42' North Latitude and 75° 30' West Longitude.

are morphologically consistent with the presence of permafrost. A number of other features associated with cold-climates, including dunes, sand sheets and shallow depressions noted in the area, are considered to have formed during the coldest part of the Wisconsinan glaciation (Lemke et al., 2004).

The generally-accepted origin of ground wedges or ice-cast wedges in the coastal plain is thermal contraction of perennially-frozen ground with cracks infilled with aeolian sands frosted and deposited by strong katabiatic winds. Modern analogs in high latitudes indicate that surface soil temperatures may have been in the -15 to -20 °C range when this cracking occurred. OSL dating of sands infilling these cracks and forming the wedges suggest a tri-modal formation chronology with wedges forming at >147 ka, again at 50 to 70 ka and a more recent set at 13 to 35 ka. These ages suggest wedge formation of probable Illinoian, early Wisconsinan and late Wisconsinan age. The late Wisconsinan episode likely followed the Last Glacial Maximum (LGM) and may not be associated with significant ground ice growth. It is thought that the post-LGM episode was characterized by thin or discontinuous permafrost or deep seasonal frost. The late Pleistocene-Holocene transition has been described to have been a time of significant aeolian activity dominated by braided fluvial systems with the formation of dunes and deflation hollows on

upland surfaces (French et al., 2007).

Murton et al. (2000) discuss the formation of wedge structures by infilling of thermal contraction cracks or ice wedges. These cryogenic sand wedges are reported to occur widely in polar desert and tundra. The fill in these wedges is reported to be either massive or laminated and may contain pebbles and inclusions of the surrounding parent material. Large wedges exceeding 2 m in depth are interpreted as being evidence of continuous permafrost. Many wedges are reported to have been morphologically modified by post-depositional forces such as loading, slope-related movement, glaciotectonic deformation or frost heaving.

Markewich et al. (2009) report parabolic dunes of aeolian origin on the west shore of the Chesapeake Bay that have their origins in the Wisconsinan glaciation. They report a recent episode of significant aeolian deposition that coincides with the period of major growth in the Laurentide Ice Sheet between 35 and 15 ka. Three or more intervals during this time period saw wind as the dominant geomorphic agent in this region. Each of these episodes are reported to have followed rapid incision into crystalline bedrock by the Potomac and Susquehanna rivers between 35 and 30 ka, which would have provided significant quartz as raw material for the deposition of sand across the region.

Periglacial features have been recognized in the northeastern United States for some time. Boulder rings, boulder stripes and rubble on ridge tops are reported in northern Pennsylvania and described as being a result of deep seasonal freeze and thaw during early Wisconsinan glaciation. Estimated frost depths were within 2 to 3 m at the time of formation of these features (Denny, 1951). Clark (1968) described sorted polygonal pattern ground at high elevations in Pennsylvania, West Virginia and Virginia as being periglacial in origin. These features are easily compared with modern analogues at high latitudes, such as those noted in the Devon Plateau of Nunavut in Canada (Ugolini et al., 2006).

Quaternary paleosols in the Arctic that were exposed during glacial periods exhibit relict cryogenic features including sand wedges, ice wedge casts, sand involutions and cryoturbation. Holocene soils in the same area exhibit patterned ground as the most common relict feature. The Wounded Knee Paleosol in the central Yukon, found at elevations of less than 1000 m is considered to be of early Pleistocene origin. This paleosol is strongly weathered and rubefied and exhibits a paleoargillic Bt horizon with thick argillans as well as sand wedges, ice wedge casts and ventifacts. Patterned ground and stone circles are also reported. Taarnocai & Valentine (1989) reported that the rubefication exhibited requires a mean annual air temperature (MAAT) of >7 °C. As this area now has a MAAT of -5 °C, the rubefication is interpreted as being relict.

In northwestern Europe, common Quaternary periglacial features include ice-wedge casts, cryoturbation and patterned ground. Interglacial paleosols commonly exhibit weakly rubefied argillic horizons that are thicker and more enriched in illuvial clays than those formed in the Holocene. Expulsions of air bubbles during thawing are thought to produce large rounded or mamillated pores or vesicles within these paleosols. Quaternary alterations of glacial and interglacial sediments could be stronger in the middle latitudes, resulting in relict features that are more widespread (Catt, 1989). Permafrost degradation is reported to produce thaw consolidation and liquefaction that contributes to a compacted layer at the level of the paleo-permafrost table (French et al., 2009). Paleosols such as these can provide information on past climatic histories. Investigations of loess-paleosol sequences in Southeastern Central Europe and Central China have provided detailed climatic information on portions of the middle and upper Pleistocene. These interpretations must be made carefully, however, as many paleosols are truncated (Bronge and Heinkele, 1989).

Based upon this growing body of information, it is not unreasonable to expect to find evidence of periglacial impact on sites farther south than previously documented. The objective of this study was to identify and document a paleosol and landform features and to determine if their origin is periglacial.

Table 1. Profile log for test pit 1411 described using the USDA system. The Ap and C horizons consist of loose and relatively structureless aeolian sands overlying the surface of the paleosol (2Btg horizon) and lower horizons of varying parent materials. Note the change in consistency starting at the 2Btg horizon and continuing with depth. The plasticity of the 2Btg horizon and the firmness and massive structureless condition of the 3Btg and 4Cg horizons could indicate compaction due to consolidation and liquefaction from degradation of permafrost. The 4Cg horizon is cemented.

Horizon	Depth in inches	Matrix Color	Texture	Structure	Consistence	Boundary	Redox Feature Color	Redox Feature Description	Notes
Ap	0-12	2.5Y4/2	medium sandy loam	coarse weak subangular blocky	very friable	clear smooth			
C	12-27	2.5Y8/4	medium loamy sand	single grain structureless	loose	clear smooth			
2Btg	27-32	10YR5/6	medium sandy clay-loam	medium weak subangular blocky	slightly plastic	abrupt smooth			
3Btg	32-56	Variegated N6/ & 5R5/6	clay	medium strong subangular blocky	extremely firm	abrupt smooth	N6/	matrix	
4Cg	56-72	Variegated N8/ & 7.5YR6/8	medium sandy loam	massive structureless	extremely firm	gradual smooth	N8/	matrix	cemented
5Btg	72-97	Variegated 5PB8/1 & 7.5YR5/6	clay-loam	massive structureless	plastic	clear smooth	5PB8/1	matrix	old lignitic roots to 97"
6Cg	97-105	Variegated 10YR7/1 & 10YR5/8	felspathic heavy medium sandy loam	massive structureless	friable				

REGIONAL SETTING

The site is a 53 hectare (130 acre) tract of land located in Sussex County, Delaware, United States of America at approximately 38° 42' North Latitude and 75° 30' West Longitude (Figure 1). The site is located on the Delmarva Peninsula, in the Coastal Plain Physiographic Province of the Mid-Atlantic Region. The site was a fallow farm field dominated by weeds and surrounded to the north by a young, managed Loblolly pine forest.

Topography is gently rolling, concavo-convex and has very little topographic relief. Elevations in the area range from less than 10 m above mean sea level (MSL) along streams to more than 18 m above MSL at Wilson Hill to the northeast of the study areas.The surface drainage is primarily accommodated by drainage ditches and channelized streams. The site is punctuated by undrained depressions. The site lies along the drainage/watershed divide between the Chesapeake Bay and the Delaware Inland Bays watershed. The site is mapped as being underlain by unconsolidated fluvio-marine sediments of the Pliocene Age Beaverdam Formation (Ramsey, 2008), which overlay Miocene estuarine and marine sediments of the Chesapeake Group (Groot and Jordan, 1999).

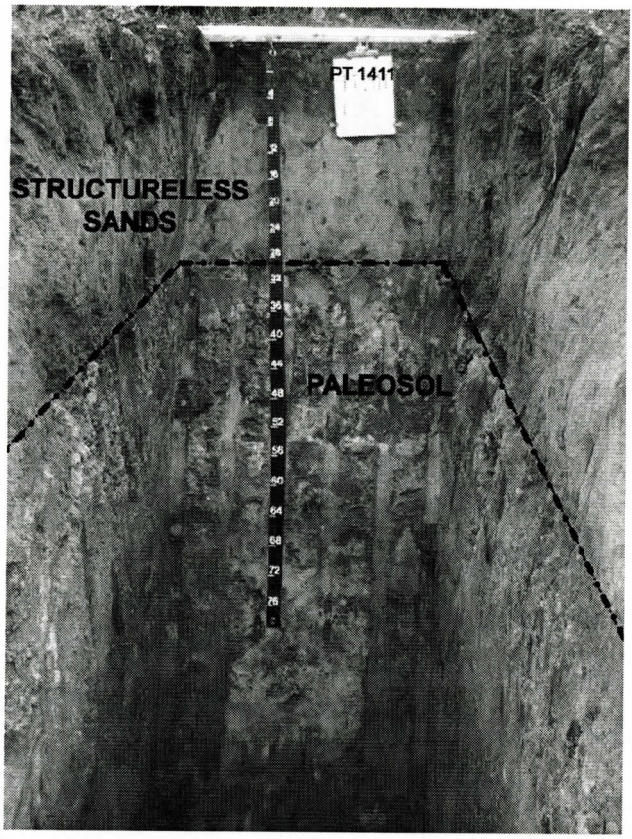

Figure 2. Test pit 1411 showing the distinct boundary between the paleosol and the overlying structureless aeolian sands.

MATERIALS AND METHODS

A preliminary reconnaissance phase consisting of 32 hand auger borings to a depth of 1.5-2.0 m was conducted using a grid pattern of 100 m across the site. The reconnaissance phase was followed by intensive, high-definition soil and hydrogeologic mapping of two areas within the property. The detailed mapping included excavation and examination of 32 backhoe pits to 4-m depth and over 325 hand auger borings at depths of 1.5 to 2.0 m on a 23-m grid pattern across the areas. The soil mapping was coupled with hydrogeologic mapping that included 33 deep probes using a direct-push rig with continuous sampling to depths of 7 to 15 m, as well as 32 deep hand auger borings completed with 5 cm diameter PVC observation wells and 11 shallower wells within the vadose zone. Soil profiles were logged using the USDA and USCS systems. Surface topography and all sample locations were surveyed in Delaware State Plane Coordinates using a combination of a survey-grade global positioning system (GPS) and conventional survey techniques allowing control of both physical locations and topography.

RESULTS AND DISCUSSION

Early examination of the soils exposed in the backhoe pits revealed that the subsurface stratigraphy of the study site was significantly more complex than anticipated based on soils and geologic maps previously published. One soil profile (Table 1) exhibited six different sets of parent materials. The surface soils consisted of relatively structureless sandy loams and loamy

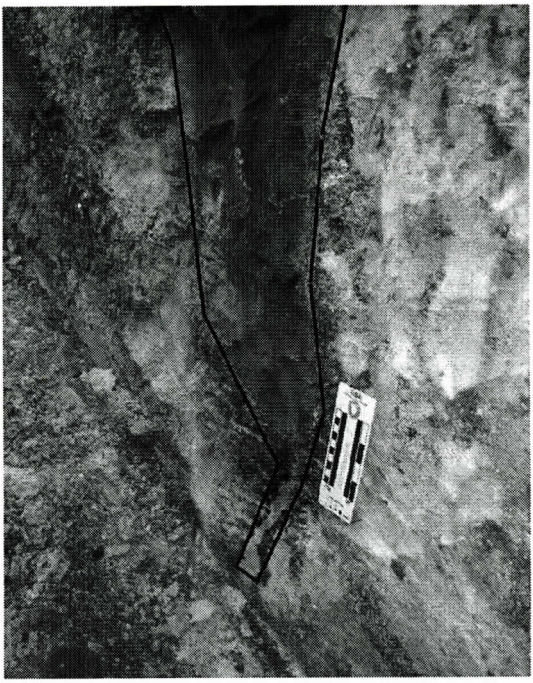

Figure 3. Test pit 1414 exhibiting wedge cast. Material within wedge is friable, massive, medium loamy sand; surrounding matrix is coarse loam to sandy clayloam.

sands that include small sub-rounded gravels overlying the paleosol, which was composed of slightly rubified and, in some cases, gleyed sandy clayloam. The lower horizons included parent materials of apparent structureless clays, lag deposits of possible aeolian pavement, fluvial trough and planar cross-stratified sands, and laminated fine to very fine sands in normal graded sets 30 to 60 cm thick, often truncated by the overlying set of beds (Figure 2). As the paleosol was encountered in nearly every test pit and auger boring, it became a focus of the investigation as it appeared that it could significantly impact subsurface water flow within the vadose zone.

The paleosol was readily recognized in both auger borings and test pits based upon color change, textural change, and induration. Subsequent infiltration testing indicated that the permeability of the paleosol was roughly 30% that of the overlying sands. Double ring infiltrometer (ASTM standard D3385-94) testing yielded an average infiltration rate of 15.86 cm/hr for the shallow soils and 4.62 cm/hr for the paleosol. This dichotomy in permeability rates mirrors initial estimations based upon soil texture, structure and consistence.

The surface of the paleosol occasionally included sub-rounded fine gravels of chert that appeared to be wind abraded. The paleosol was intersected by a number of features of interest. Two instances of apparent wedge casts were observed. The most striking wedge cast (Figure 3) was infilled with a friable, massive, medium sandy loam that was significantly more oxidized than the matrix of the paleosol. The presence of these wedge casts indicate that periglacial conditions with deep seasonal frost or permafrost existed in this region at some time in the past. We interpret these wedges to be similar to the ice wedge casts described by French, et al. (2001, 2003, 2007, 2009) or the cryogenic sand wedges described by Murton et al. (2000). The presence of the gravels at the interface between the paleosol and the surface horizons indicate that the surface of the paleosol was formed during subaerial exposure and was at one time a stable land surface, but experienced

Figure 4a. Lignitized roots are truncated at the surface of the paleosol.

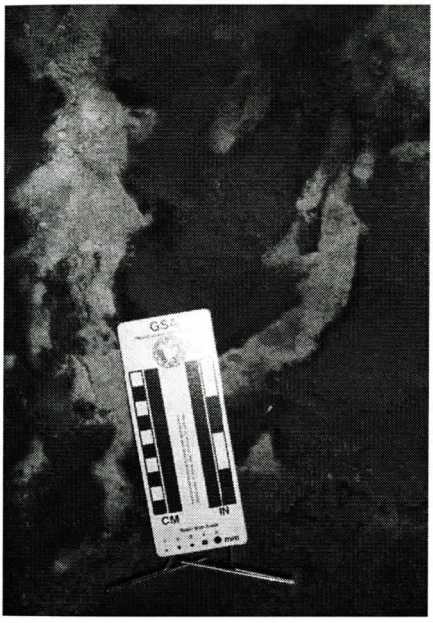

Figure 4b. Macropores in test pit 1444, which are roughly cylindrical in cross section. These could be sand wedges that have undergone post-depositional soft sediment deformation. The resemblance to rodent burrows, however, suggests that these are krotovina of animal origins. Material infilling krotovina is composed of friable, massive, medium loamy sand similar to the sands found in the surface horizons. The surrounding matrix is medium sandy loam to sandy clayloam.

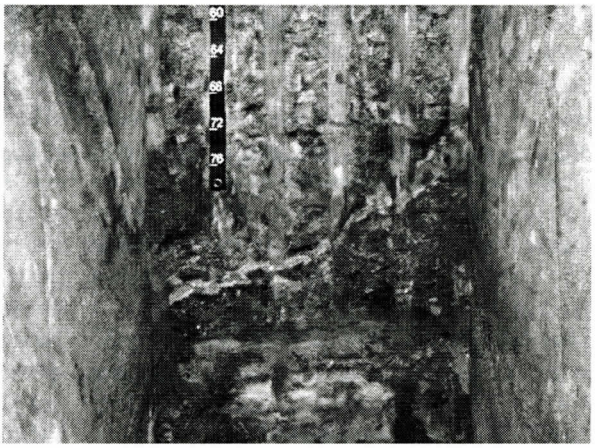

Figure 4c. Macropores of indeterminate origin. These macropores appear to be significant preferential flow pathways allowing groundwater recharge.

differential erosion and loss of all or part of a surface horizon containing gravelly clasts.

Lignitized roots that originated within the paleosol were found at a number of locations (Figure 4a). Future studies could include sampling of the roots to allow for radiocarbon dating. Significant macropores infilled with material differing from the matrix of the paleosol were recognized. The most striking of these was a series of 3 to 6 cm diameter macropores that were infilled with friable, massive white sands similar morphologically to the sands found in the surface horizons (Figure 4b). They were truncated at the overlying contact with the structureless sands and are

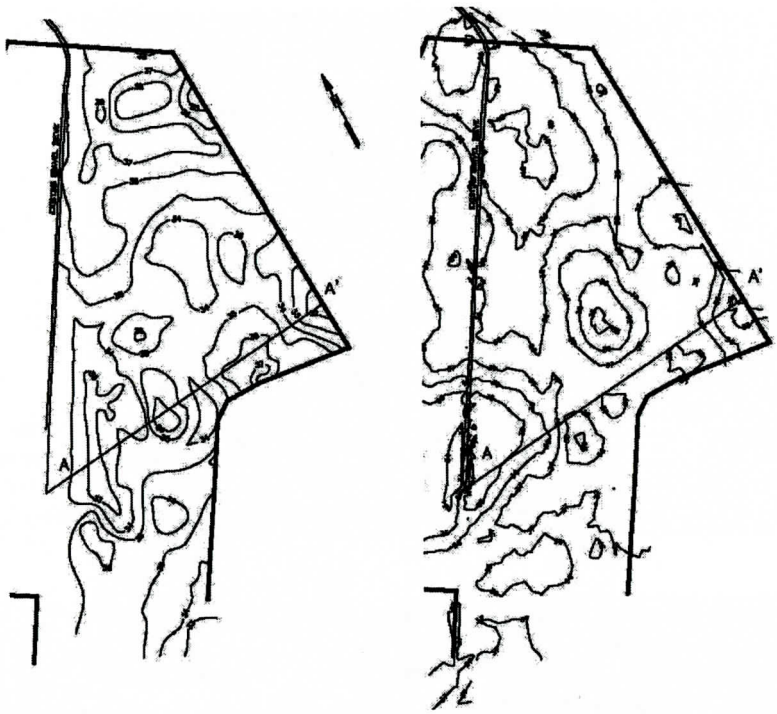

Figure 5. Isopach map comparing current surface topography (right) with paleo-topography (left). Contours are 1-foot intervals.

therefore considered post-depositional and post-date the development of the paleosol. It is possible that these features are sand wedges that have been modified by post-depositional soft sediment deformation. The shape, configuration and placement of these macropores, however, are reminiscent of rodent burrows. We hypothesize that these represent the remains of burrows inhabited by small rodents at the time when the paleosol was exposed and that these burrows were then infilled with aeolian sands as they were subsequently deposited on the site. We interpret these krotovina to be contemporaneous with the mature paleosol environment of a warm interglacial or pre-glacial period.

A number of other, less identifiable macropores were recognized in a number of locations (Figure 4c). These macropores, though their origins are less clear, are likely significant pathways for recharge of the aquifer in this area.

The systematic and detailed nature of the investigation with hand auger borings spaced on a 23-m grid pattern, coupled with precise survey location and the readily recognizable paleosol, permitted the preparation of an isopach map of the top of the paleosol. Taking the known surface elevations at each point on the grid and subtracting the depth to the surface of the paleosol yielded an elevation for the surface of the paleosol (Figure 5). We assume that this paleosol was formed during a lengthy period of subaerial exposure, that it was a stable land surface at one time and that it was subjected to modification on a macroscopic scale by alternate periods of freezing and thawing with both wind generated and fluvial erosion. Our interpretation is provisional, however, and subject to refinement as additional information becomes available. The topography of the existing land surface and the surface of the paleosol were found to differ as illustrated in the isopach map. Figure 6 illustrates the difference in the topographic profile across one area of the site.

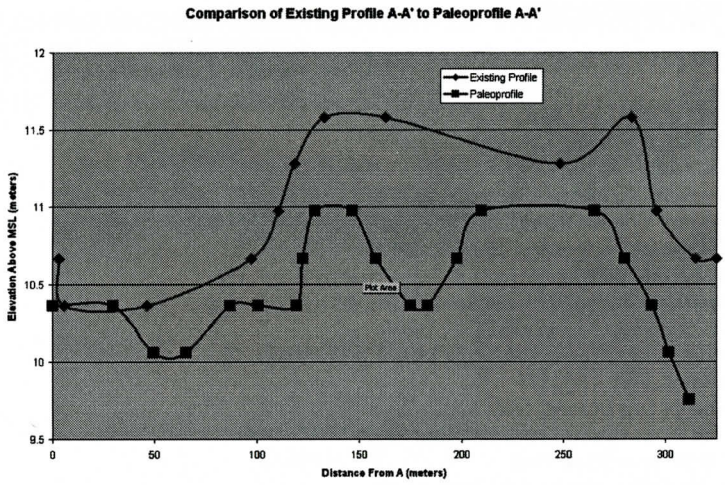

Figure 6. Profile of section A – A' comparing current surface topography with paleotopography.

CONCLUSIONS

The nature of the paleosol recognized at this site indicates that it was formed by a lengthy period of subaerial exposure followed by modification under periglacial conditions. The paleosol was subsequently buried by aeolian sands following, presumably, the last glacial event.

Wedge casts indicate periglacial influences that could be either permafrost or deep seasonal frost. Based upon the findings of French et al., the age of these ground wedges could coincide with one of the three periods of wedge formation which would place the age of the paleosol surface at >147 ka, 70 to 50 ka or 35 to 13 ka. If we assume that the paleosol was a stable land surface, this would place the age of the formation of the surface at a time previous to the latest, but most likely the oldest, glacial period. As the Beaverdam Formation is dated as Pliocene, it is also possible that this paleosol is of Pliocene origin.

The significance of aeolian processes as a result of katabiatic winds in the formation of the landscape of the Coastal Plain has been documented repeatedly by others. The presence of structureless sands with a relative lack of significant pedologic development in the surface horizons is consistent with this model. The wind abraded gravels found within the sands above the paleosol and at the surface of the paleosol support an aeolian origin for the sands resting on the surface of the paleosol. An aeolian origin is consistent with the existing undrained depressions on the site that appear to be formed as deflation hollows. We interpret some of the macropores noted in profiles as the remnants of animal burrows. Some other macropores appear to be krotovina of plant origin or of undetermined origins.

We suggest the existence of a buried landscape that pre-dates the glaciations of the Pleistocene. We further suggest that this landscape was formed under a warmer, non-glacial climate during the Pliocene and remained relatively stable through much of the Pleistocene. This land surface was strongly influenced by periglacial processes including permafrost or deep seasonal frost during episodes of continental glaciations as evidenced by wedge casts. During interglacial periods, this landscape was vegetated and inhabited by fauna as evidenced by the macropores encountered. The land surface was repeatedly impacted by aeolian scouring, sedimentation and modification/alteration due to strong katabiatic winds of glacial origin. These aeolian depositional episodes are likely responsible for burying the area under structureless sands which also infilled the wedges and faunal krotovina creating the gentle topography that exists today.

REFERENCES

Andres, A.S. and Howard, C.S.; Analysis of Deformational Features at the Pollack Farm Site, Delaware; Geology and Paleontology of the Lower Miocene Pollack Farm Fossil Site, Benson, R.N. (eds). Delaware Geological Survey, Special Publication No. 21, 47-53, 1998.

Bronge, A. and Heinkele, K., Paleosol Sequences as Witnesses of Pleistocene Climatic History; CATENA Supplement 16, Paleopedology, Nature and Application of Paleosols, pp. 163-186, 1989.

Catt, J., Relict Properties in Soils of the Central and North-West European Temperate Region, CATENA Supplement 16, Paleopedology, Nature and Application of Paleosols, pp. 41-58, 1989.

Clark, M.G.; Sorted Pattern Ground: New Appalachian Localities South of the Glacial Gorder; Science, Vol. 161, Number 3839, pp 355-356, 1968.

Denny, C.; Pleistocene Frost Action Near the Border of the Wisconsin Drift in Pennsylvania; The Ohio Journal of Science, Vol. 51 (3), May 1951.

French, H.M. and Demitroff, M.; Cold-climate Origin of the Enclosed Depressions and Wetlands ('Spungs') of the Pine Barrens, Southern New Jersey, USA; Permafrost and Periglacial Processes, Vol. 12:337-350; 2001

French, H.M., Demitroff, M. and Forman, S.L.; Evidence for Late-Pleistocene Permafrost in the New Jersey Pine Barrens (Latitude 39^0 N), Eastern USA; Permafrost and Periglacial Processes, Vol. 14:259-274; 2003.

French, H.M., Demitroff, M., Forman, S.L. and Newell, W.L.; A Chronology of Late-Pleistocene Permafrost Events in Southern New Jersey, Eastern USA; Permafrost and Periglacial Processes, Vol. 18:49-59; 2007.

French, H.M., Demitroff, M. and Newell, W.L.; Past Permafrost on the Mid-Atlantic Coastal Plain, Eastern USA; Permafrost and Periglacial Processes, Vol. 20:285-294; 2009.

Groot, J.J. and Jordan, R.R.; The Pliocene and Quaternary Deposits of Delaware: Palynology, Ages, and Paleoenvironments; Delaware Geological Survey Report of Investigations No. 58, 1999.

Lemke, M.D. and Nelson, F.E.; Cryogenic Sediment-Filled Wedges, Northern Delaware, USA; Permafrost and Periglacial Processes, Vol. 15:319-326; 2004.

Markewich, H.W., Litwin, R.J., Pavich, M.J. and Brook, G.A.; Late Pleistocene eolian features in southeastern Maryland and Chesapeake Bay region indicate strong WNW-NW winds accompanied growth of the Laurentide Ice Sheet; Quaternary Research, Vol. 71:409-425; 2009.

Murton, J.B., Worsley, P. and Gozdzik, J.; Sand Veins and Wedges in Cold Aeolian Environments; Quaternary Science Reviews, Vol. 19:899-922; 2000.

Ramsey, K.W.; Delaware Geological Survey, personal communication, 2008.

Tarnocai, C. and Valentine, K.W.G., Relict Soil Properties of the Arctic and Subarctic Regions of Canada, CATENA Supplement 16, Paleopedology, Nature and Application of Paleosols, pp. 9-39, 1989.

Ugolini, F.C., Corti, G., and Certini, G., Pedogenesis in the Sorted Pattern Ground of Devon Plateau, Devon Island, Nunavut, Canada, Geoderma Vol. 136, pp. 87-106, 2006.

SOUTHEASTERN GEOLOGY
V. 47, No.2, May 2010, p. 95-104

THE HOLOCENE DEPOSITIONAL HISTORY OF THOUSAND ACRE MARSH (GEORGETOWN COUNTY, SC, USA) FROM CORRELATION OF GROUND PENETRATING RADAR WITH SUBSURFACE STRATIGRAPHY

A. SPRINGER

Department of Geological Sciences
University of South Carolina
Columbia, SC 29208
aspringer@geol.sc.edu

CAMELIA KNAPP

Department of Geological Sciences
University of South Carolina
Columbia, SC 29208

PAUL T. GAYES

Center for Marine and Wetland Studies
Department of Marine Science
Coastal Carolina University
Conway, SC 29526

LEONARD R. GARDNER

Department of Geological Sciences
University of South Carolina
Columbia, SC 29208

ABSTRACT

Thousand Acre Marsh, near Georgetown, SC has been investigated using ground penetrating radar and auger cores to determine this brackish marsh's recent depositional history. Core lithology, wood samples, vegetation fragments, and geophysical horizons all aided in the construction of a stratigraphic framework and the identification of antecedent environmental changes and the formation of Thousand Acre marsh, North Inlet-Winyah Bay, SC with regard to recent sea-level rise.

INTRODUCTION

Brackish marshes are diverse coastal environments situated at the apex between saltwater and freshwater systems. These marshes can be a key in identifying Holocene sea-level fluctuations. These coastal environments are more susceptible to changes in sea-level than their salt water counterparts. Analyses of brackish marsh subsurface facies and lateral extent can provide indications and timing of Holocene sea-level fluctuations.

Ground Penetrating Radar (GPR) is a non-intrusive, high-resolution method for detecting and mapping subsurface geological features *in situ*. It is widely used in geophysical site characterization studies because it allows for excellent documentation of the lateral extent, continuity, depth, and thickness of the subsurface units in areas where the soil and shallow strata have low conductivity (Neal, 2004).

Brackish marshes are challenging environments for GPR studies due to attenuation of the electromagnetic signal by salt water saturated sediments and clay deposits (Neal, 2004). A previous investigation by Weaver (2006) showed that interpretable GPR data could be obtained from brackish marshes in South Carolina In the Weaver (2006) study, the electro-

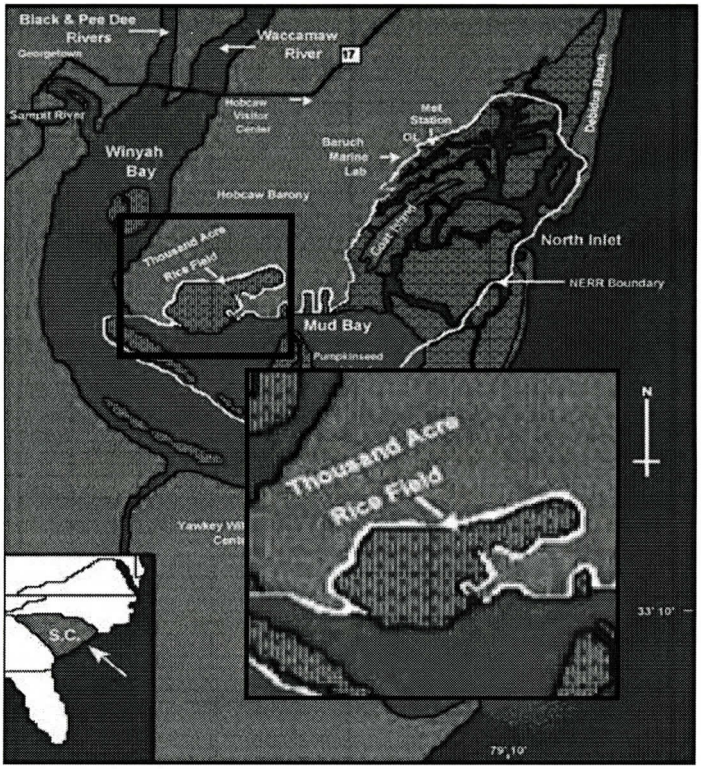

Figure 1. TAM is located east of Georgetown, SC and west of North Island and North Inlet within the NOAA-NERRS and Hobcaw Barony property. Figure has been modified from www.northinlet.sc.edu; the Baruch Marine Field Laboratory is part of NOAA_NERRS.

magnetic signal had significant penetration through shallow clay deposits.

The present investigation utilizes GPR images and sediment cores to aid in facies identification, lateral facies extent, and determination of depositional units for correlation of radar reflectors observed in the GPR data in Thousand Acre Marsh, Georgetown County, SC. The combination of these proxies could aid in the deciphering of Holocene sea-level and the effect on coastal environments.

The documented Holocene sea-level rise of 3 mm/yr on the South Carolina coast (Colquhoun, 1969), is altering the geomorphology of shorelines and coastal environments (DePratter and Howard 1981; Gayes and Scott, 1992; Gardner and Porter, 2001; Baldwin, *et al.*2004). The Holocene stratigraphy of brackish marshes should be investigated to increase our knowledge of antecedent sea-level fluctuations and to forecast the future of our coastal resources in relation to rising sea levels.

In South Carolina coastal environments, GPR has been used to investigate Holocene stratigraphy of barrier islands to determine the formation and evolution of these sand systems (Wright et al., 2006). GPR has also been used in the Santee State Park located in Santee, SC, to locate sinkholes within the Santee Limestone that were causing extreme road damage (Addison et al., 2008). In addition, GPR has been utilized often for lithological characterization, such as identification of facies variations and extent within the subsurface (Addison, 2006; Weaver, 2006).

The objectives of this multidisciplinary investigation of the Thousand Acre brackish marsh system include: 1) correlation of the subsurface stratigraphy from analyses of sediment cores with high resolution, non-invasive GPR imaging techniques; 2) determination of the recent depositional history of TAM based only on

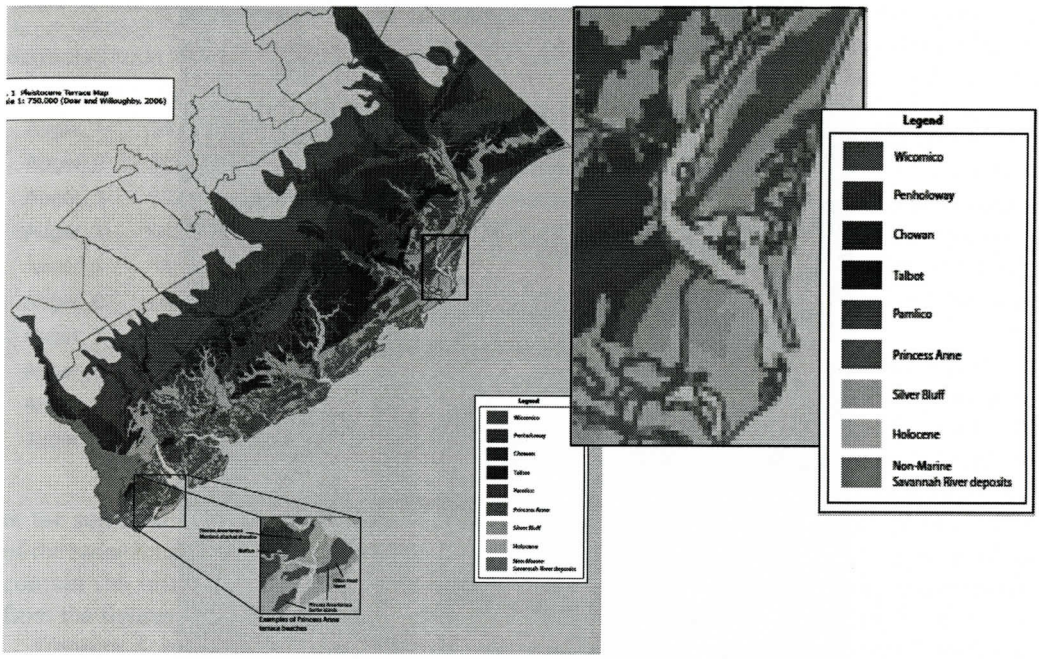

Figure 2. Location of sampling Thousand Acre Marsh GPR transect locations. Transects are represented by black lines. Transects A and A_200 are on the right hand side while transect B runs perpendicular to A and C. C is the western line that runs parallel to A and A_200.

the above mentioned analyses and 3) presentation of these data for future recommendations of sea-level management in these important coastal environments.

STUDY SITE

Thousand Acre Marsh is located northeast of Georgetown, SC, within the National Oceanic and Atmospheric Administration – National Estuarine Research Reserve (NOAA-NERRS) North Inlet-Winyah Bay (NI-WB) site and the Belle W. Baruch Institute for Marine & Coastal Sciences at Hobcaw Barony (Figure 1). This site is a low-lying area with an average elevation 0.5 m above mean sea level (msl), surrounded to the west by relict, 100-80 ka, Pleistocene Princess Anne Formation beach ridges, which average 15 m above msl (Doar and Kendall, 2008). To the north and east of Thousand Acre Marsh, is a younger set of 60-30 ka beach ridges, averaging 3 m above msl, known as the Silver Bluff Formation (Doar and Kendall, 2008) (Figure 2). Thousand Acre Marsh is located in a temperate to subtropical climate with a mean annual temperature of 18°C and an average precipitation of 130 cm/yr. Thousand Acre Marsh is a brackish marsh subject to an average tidal range of 1.5 m. The main vegetation is *Spartina juncus* and *Spartina cynosuroides,* more commonly known as Bullrush and Big Cordgrass, respectively (DeVoe and Vernberg, 1992).

METHODS

Geophysical Data Acquisition

Ground Penetrating Radar (GPR) data were acquired using the Pulse EKKO 100 system manufactured by Sensors and Software, Inc. Five transects, using the common offset method, were acquired across the southern portion of Thousand Acre Marsh. These transects will aid in determining subsurface geometry and underlying depositional sequences. This GPR system operates with a transmitting antenna and receiver which were spaced according to the chosen antenna size.

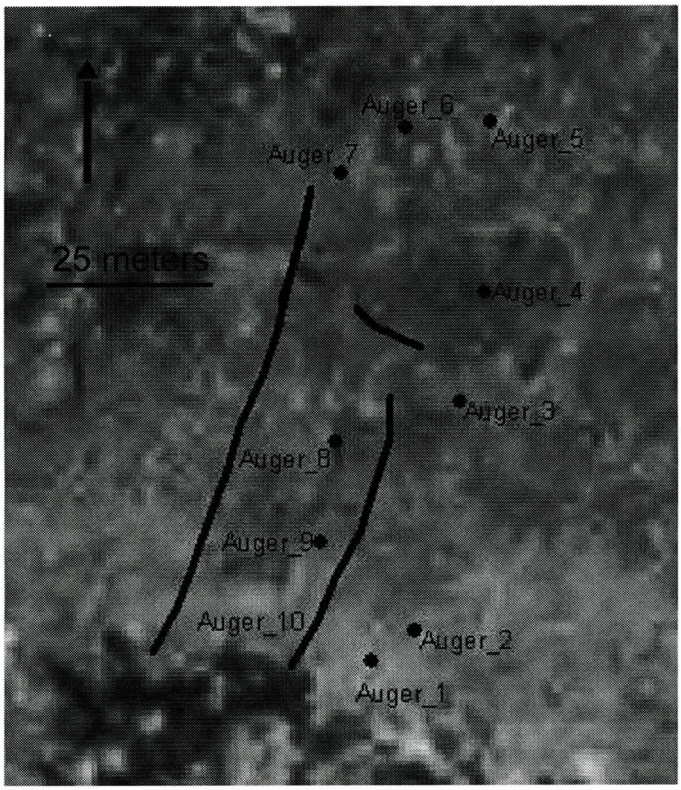

Figure 3. Black lines represent the locations of the GPR transects with respect to the sediment cores, for further information on GPR locations see figure 3. Auger cores are represented with circles, push cores by triangles and squares for vibracores. Figure modified from USDA ADAR image through ArcGIS version 9.

Over 300 meters of GPR transects were acquired. Transect A begins north of the embankment road on the Winyah Bay side and heads north into the marsh. Transect B begins at the end of Transect A and proceeds to the west towards transect C. Transect C begins further into the marsh than Transect A but follows a parallel path back toward the embankment road (Figure 3). Transect A was also examined with a 200 mHz antenna (A_200).

Imaging of approximately 4 m into the subsurface of TAM was possible from the acquired GPR data. This is due to the electrical properties of geologic material (Topp et al., 1980; Davis and Annan, 1989; and Wilson, 1998).

Sediment Core Acquisition

Ten auger cores were acquired for ground truthing and correlation with the GPR data. (Figure 3). Auger cores were extracted at 1 meter length segments with a handheld auger and recorded in the field. Samples of distinction were sealed in containers and frozen for future analyses. Core locations and lengths are recorded in Table 1.

RESULTS

Ground Penetrating Radar

Over 300 meters of Ground Penetrating Radar (GPR) data were acquired along Thousand Acre Marsh transects A-C. Attenuation of a portion of the GPR signal in this environment occurred due to salt water intrusion into the sediments and the presence of clay sediment. Some interference occurred in transects A and C due

Table 1. The table provides the location and depth without compaction of all sediment cores extracted from Thousand Acre Marsh (TAM).

Core ID	Easting	Northing	Depth (cm)
Auger_1	662301	3685896	100
Auger_2	662310	3685902	100
Auger_3	662319	3685948	98
Auger_4	662324	3685970	133
Auger_5	662325	3686004	389
Auger_6	662308	3686003	100
Auger_7	662307	3686003	280
Auger_8	662295	3685994	240
Auger_9	662294	3685940	159
Auger_10	662291	3685920	100

to the surrounding forest. The deeper portions of the radar images of transects A and C which contain the interference have been removed from the figures.

Transect A is 72 meters in length, and was acquired with a 100 mHz antenna (Figure 4). The radargram reveals the majority of the beds are flat-lying but there is visual evidence of radar reflections that are highlighted in Figure 4. The radar reflectors in Transect A are located at depths of: 0.75, 1.5, 3 and 4.5 meters.

Transect A_200, 34 meters of Transect A, was acquired with the 200 mHz antenna (Figure 5). The resolution is much improved with the 200 mHz antenna, but depth of penetration is limited. The radar reflectors in Transect A_200 are located at depths of: 0.75 and 1.7 meters.

Transect B, acquired with a 100 mHz antenna, is 30 meters in length and connects Transects A and C from east to west (Figure 6). The radar reflectors of this transect occur at depths of: 0.8, 2 and 3 m.

Transect C is 107 m in length from North to South and was acquired with a 100 mHz antenna. Transect C (Figure 7) correlates well with transect A, which it parallels from North to South. Radar reflectors can be seen at depths of: 0.75, 2, 3.2 and 4.6 meters within Transect C.

All transects and corresponding images that were acquired with the 100 mHz antenna contain distinct radar reflectors. These horizons can be seen in transects A, B and C and Table 2. Radar reflectors in each transect are located at average depths of 0.75, 1.7 and 3 meters depths. The slight disparity of these radar reflector depths in each transect can be attributed to lateral variation due to natural processes such as creeking, erosion and varying sediment distri-

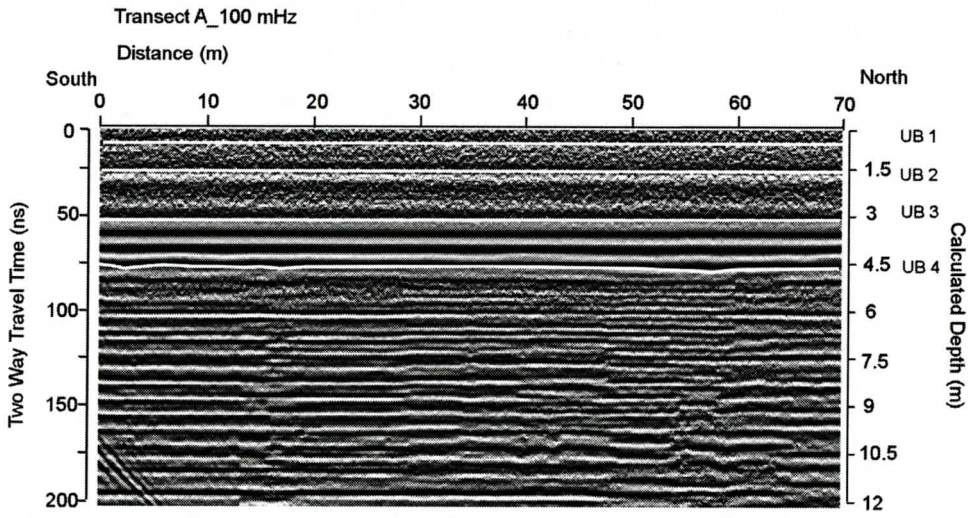

Figure 4. Transect A was acquired with a 100 mHz antenna beginning at the southern portion of the basin headed north into the marsh. The depth scale is based on the assumed velocity of 0.06 m/ns which is considered to be the velocity of the EM wave through wet clays and sands. Unit boundaries are displayed by arrows.

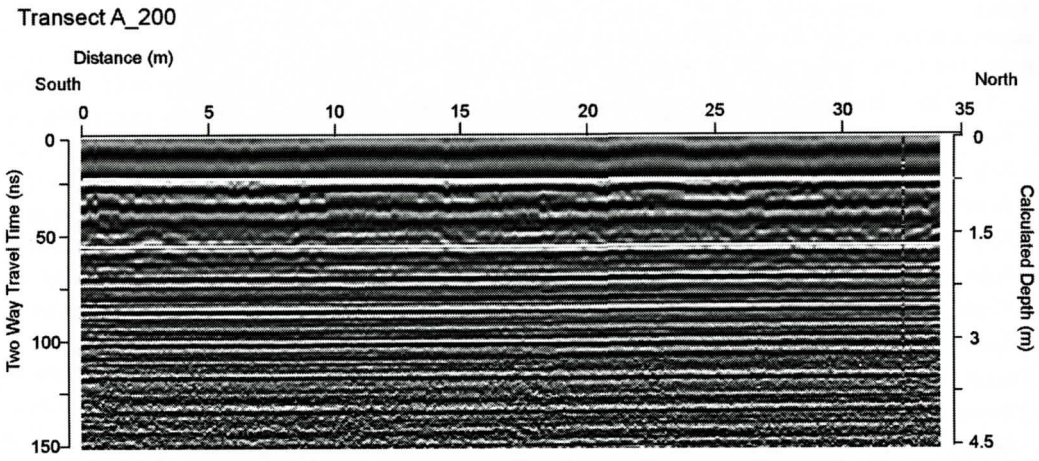

Figure 5. Transect A_200 acquired with the 200 mHz antenna. The depth of penetration is more limited than with the 100 mHz antenna. Unit boundaries are marked by arrows.

Table 2. Depth of geophysical horizons identified within the acquired GPR transect images.

Transect ID	Horizon 1 Depth (Meters)	Horizon 2 Depth (Meters)	Horizon 3 Depth (Meters)	Horizon 4 Depth (Meters)
Transect A	0.75	1.5	3	4.5
Transect A_200	0.75	1.7		
Transect B	0.8	2	3	
Transect C	0.75	2	3.2	4.6

bution. Transect A_200 which was acquired with the 200 mHz antenna has a higher resolution radar image but lacks the penetration depth of the 100 mHz antenna. Thus, transect A_200 reveals only 2 distinct geophysical horizons at depths of: 0.75 and 1.7 meters, but contains much more detail within these units.

Cores

Ten auger cores were collected, ranging in depth from 98-389 centimeters to ground truth GPR transect data and radar reflector depth and to construct a stratigraphic framework. Figure 8 is a representation of Thousand Acre Marsh stratigraphy based on core analyses. The near surface sediments of the marsh are a thickly vegetated mud typical of a vegetated brackish marsh and will are referred to as Facies 1 (Figure 8). This deposit, termed 'modern marsh' facies, is a brown mud (10YR 2/2) with root mats from the Big Cordgrass, *Juncus cynosuroides.* The 'modern marsh' facies was identified in all cores and ranged in thickness from 20 cm to 45 cm.

Facies 2 is identified by gray clay (5Y 4/1) with interspersed degraded vegetation and is found in all cores. This facies has much less vegetation than the overlying unit and the amount that is present has been highly degraded. The high clay content suggests a quiet environment where the small clay grains settle out of the water column. Thus, Facies 2 could be interpreted as similar to Facies 1 and has either been compacted and vegetation has had a chance to decay due to diagenesis or Facies 2 had a greater freshwater influence and the slight lessening of salinity allowed for different vegetation to flourish.

Facies 3 is a dense gray clay layer and averages 25 cm in thickness. The clay consistency in this facies is much denser, suggesting a deepening of quiet water allowing for the smallest of clay grains to settle from the water column. Fa-

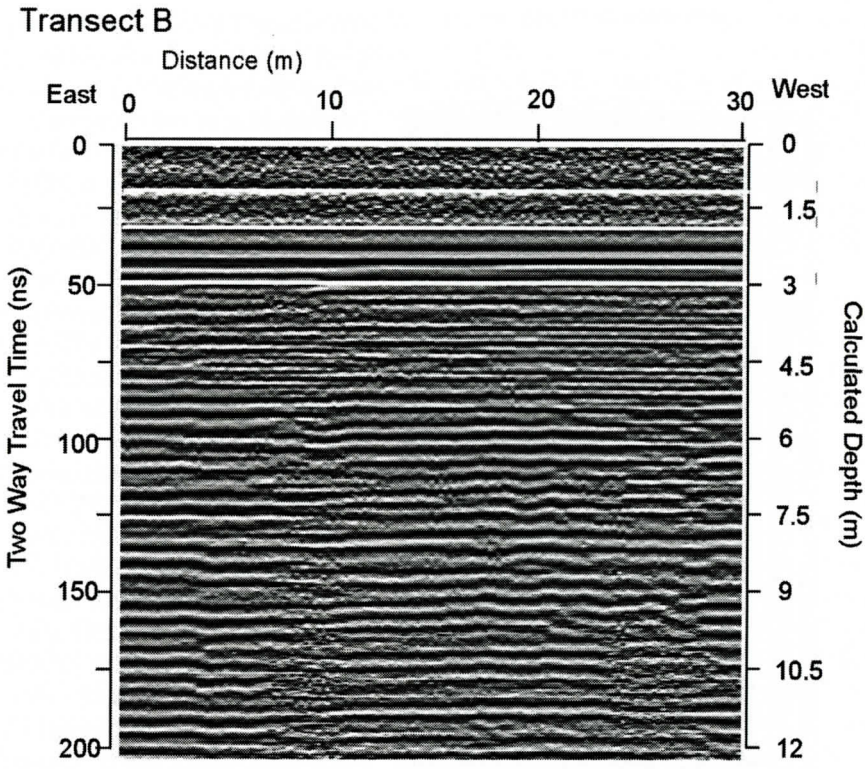

Figure 6. Transect B was acquired from east to west and connects Transect A to Transect C. Depth was determined by D=(v*(TWT/2)) and the average EM wave velocity within saturated clays and soils. Unit boundaries are marked by arrows.

cies 4 is a poorly sorted, orange-brown to tan sand layer which represents a drastic environment change from the overlying clay sediments.

Auger cores 1-3 all terminate in a gray sandy clay at 100cm depth, Facies 5, which could represent a fluvial channel bend, crevasse splay or floodplain, as evidenced by a mix of clay and sand at 80-100 cm. Auger cores 5, 7 and 8 all recovered an average 100 cm of dark black/gray to black clay that contains numerous large black wood fragments, (Facies 6). These same auger cores terminate in dark gray/ black clay with red cedar wood fragments (Facies 7) appearing at depths of 220-390, with an average thickness of 130 cm. Facies 7 may represent a period of time when a freshwater swamp influenced TAM, as evidenced by the presence of the cypress tree fragments. Cypress trees are commonly found in southeastern freshwater wetlands such as freshwater swamps and floodplains (Montane, 2007).

DISCUSSION

The main objectives of this investigation of Thousand Acre Marsh were to utilize sediment core lithology to ground truth GPR transects and to provide knowledge of Thousand Acre Marsh's recent depositional history. The impedance character of different substrates reflect and scatter the GPR signal in order to provide an average depth for GPR unit boundaries and correlation of sediment cores. Four radar reflectors were identified from the GPR images within in the TAM study area at average depths of 0.7, 1.7, 3 and 4.5 meters (Figures 4-7).

The first radar reflector at an average depth of 0.7 meters does not directly correlate with any of the lithologic changes in the stratigraphic framework from sediment core analyses, but could represent the water table. The second radar reflector located at an average depth of 1.7 meters correlates with a lithological boundary

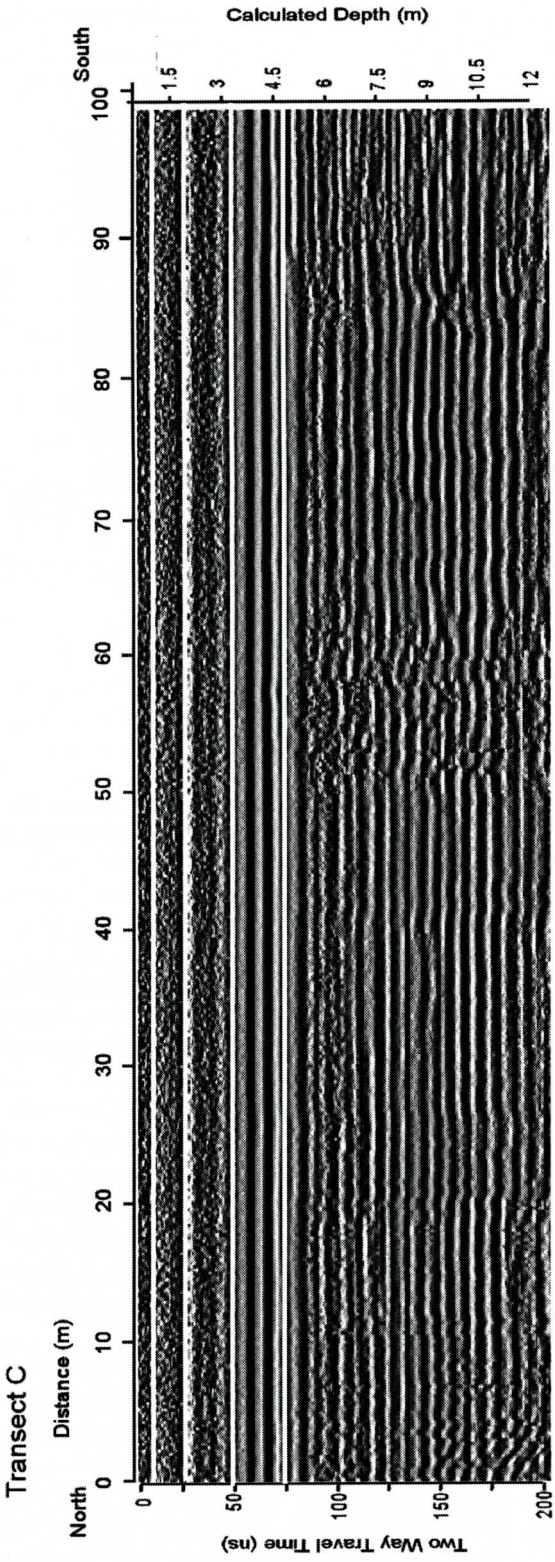

within Auger Core_5 which changes from dense peaty clay to olive black clay with large wood fragments (facies 3 to facies 5). The inclusion of wood fragments suggests either a freshwater environment where trees could survive or a location that trapped wood fragments such as a riverbank, delta or riverbend. All of these environments suggest freshwater influence much greater than the present. Thus, this second radar reflector could represent an older freshwater environment, possibly a floodplain. The presence of a previous freshwater environment is evidenced by several other studies, including the presence of tree stumps near Bly Creek located northeast of the current investigation (Gardner and Porter, 2001). Montane (2007) located three freshwater peat samples at 1.11, 2.16 and 2.41 meters depth within cores from a North Inlet salt marsh island Baldwin (2002) using a sub-bottom profiler, located a paleochannel offshore of North Inlet, which led the investigation to contemplate if that channel was the ancestral PeeDee River channel justifying the presence of these freshwater environments at a much lower sea level.

The third GPR radar reflector is located at an average depth of 3 meters. Analyses of the auger cores identified a lithological boundary at 3.2 meters that separates black clay with wood from black clay with fragments of wood that are red. The red wood fragments suggest a freshwater Cypress-Tupelo swamp, which are common along the southeastern coastal states and portray a much lower sea level then present. A present day example would be Congaree Swamp, a floodplain swamp of the Congaree River outside of Columbia, SC. Core lithology associated with the fourth radar

Figure 7. Transect C was acquired from North to South within the TAM basin. Depth was determined by D=(v*(TWT/2)) and the average EM wave velocity within saturated clays and soils. Unit boundaries are marked by arrows.

reflector cannot be used for ground truthing because sediment from that depth could not be retained with the auger core. However, previous investigations have discovered evidence of relict sand dunes from the ancient barrier island systems of Princess Anne and Silver Bluff highstand formations (Doar and Kendall, 2008; Gardner and Porter, 2001).

The combination of core lithology, sediment stratigraphy and geophysical images and horizons have aided in the interpretation of the depositional history of Thousand Acre Marsh. The facies reveal gradual changes from a possible relict dune swale-forest-river floodplain-freshwater swamp-freshwater marsh-brackish marsh due to the recent inundation of saltwater into this low lying marsh. Doar and Kendall (2008) suggest that TAM could be the result of a low-lying area located between to relict barrier islands which represent highstand shorelines. During the Pleistocene, this area was a swale between the former Princess Anne barrier island system, deposited ~100-80 kya and the later Silver Bluff barrier island system, deposited ~ 60-30 kya. The relict dune systems then slowly transitioned into forests and the swale became vegetated. The Pee Dee River migrated southward toward its present location during the Holocene due to the uplift of the Cape Fear Arch (Montane, 2007). The Pee Dee River could have flooded TAM creating a floodplain, then maybe a floodplain swamp as the North Island prograded southward and with it the PeeDee river, which was part of the most recent Myrtle Beach highstand barrier island system between ~135 – 120 kyrs (Dubar et al., 1974, Baldwin, 2002). There is also evidence that the Waccamaw could have flooded through North Inlet as well. Further analyses will be conducted to determine which or if both events affected Thousand Acre Marsh.

The continuation of saltwater inundation, increasing each year at an average rate of 3mm/yr (Colquhoun, 1969) is changing the dominant macrophyte from the black needlerush *Juncus roemarianus* to the grass *Spartina alterniflora.* If inundation of Thousand Acre Marsh by saltwater continues at the current rate of sea-level rise, the surrounding forest will begin to retreat up the relict dunes. As sea level continues to rise Thousand Acre Marsh could easily become flooded. The surrounding higher elevated forest area could disrupt the lateral migration of this environment and TAM would be come flooded instead of migrating. Thus, TAM could become similar to modern day mudflat environment of Mud Bay.

CONCLUSIONS

Here we present a description of the depositional history of Thousand Acre Marsh based on auger sediment cores and GPR data. The depositional history of this brackish marsh system includes the maturing of this environment 1) from a swale between relict beach ridge systems, 2) to a fluvially influenced environment by the migrating Pee Dee River and morphing from a floodplain to a floodplain swamp, and lastly 3) transitioning to the present day brackish marsh dominated by *Juncus roemarianus* related to the recent sea-level rise. Based on current trends, Thousand Acre Marsh will become inundated by saltwater as sea level continues to rise, thus, drowning and morphing Thousand Acre Marsh into a modern day Mud Bay.

Though this investigation has not been able to document specific Holocene sea-level cycles it has shown the present inundation of Thousand Acre Marsh and perhaps a forecast of future geomorphic changes to the South Carolina coast.

ACKNOWLEDGMENTS

This research was funded by a 2-year GAANN fellowship from the Department of Geological Sciences at the University of South Carolina under the guidance of Doug Williams with assistance of Sea Grant funding from Coastal Carolina University under the guidance of Paul Gayes. Numerous individuals have contributed to the completion of this research. Field workers include Alan Rickenbacker, James Hinkle, Allison Tockstein, Taylor Hudson Jessica Heffstatler and many of the members of the undergraduate Marine Science club, SEAS. I

would like to thank Brad Battista and Bob Trenkamp for bringing their specialities into my project with GPR acquisition and RTK GPS acquisition. The Belle W. Baruch Institute also aided in this investigation in many ways including aid with machinery and equipment, GIS data the history of the property and general knowledge of the environments. For all that help I would like to thank Stephen Forehand, Jenn Spicer, Paul Kenny, Jan Blakely, and Erik Smith. Lastly, I would like to thank all of the people from Coastal who have helped me out both in the field, with equipment, funding and with the whole process. These people include Dr. Paul Gayes, Dr. Jenna Hill, Jamie Phillips, Matt Howe and Julie Quinn. I would also like to thank Melissa Hollen for all of her editing.

REFERENCES

Addison A. 2006. Determining the Thickness of an Alluvial Sand Using the Ground- Penetrating Radar. African American Professors Program Monograph.

Addison A., N. Badger, B.M. Battista, C. Amos, I. Gupta, H. Park, D.M. Encui, R. Trenkamp, C. C. Knapp and J.H. Knapp, 2008. Ground Penetrating Radar (GPR): Seeking for Sinkholes at Santee State Park, Santee, SC. GSA- southeastern Section – 57th Annual Metting (10-11 April, 2008). Abstracts with Programs. 40(4), 1-10.

Baldwin W. E., 2002. Effects of Local and Regional Antecedent Geology of the Middle Inner Continental Shelf: Southern Long Bay, South Carolina. Geological Sciences. Columbia, University of South Carolina: 138.

Baldwin W.E., R.A. Morton, J.F. Denny, S. V. Dadisman, W.C. Schwab, P.T. Gayes and N.W. Driscoll, 2004. Maps Showing the Stratigraphic Framework of South Carolina's Long Bay from Little River to Winyah Bay, 2004-1013, USGS.

Baldwin, Wayne E; Morton, Robert A; Schwab, William C; *Gayes*, Paul T; Driscoll, Neal W., 2004. Modern availability and historic supply of sediment along the inner-continental shelf offshore northeast South Carolina. Abstracts with Programs - Geological Society of America, vol.36, no.2, pp.132,

Brockington L., 2006. Plantation Between the Waters, A Brief History of Hobcaw Barony. Charleston, The History Press.

Colquhoun D.J., 1969. Geomorphology of the Lower Coastal Plain of South Carolina: Division of Geology, South Carolina State Development Board, Publication MS-5, 1-36.

Davis J.L. and A.P. Annan, 1989. Ground-Penetrating Radar for High-Resolution Mapping of Soil and Rock Stratigraphy. Geophysical Prospecting. 37(5), 531-551.

Doar W. R., III and Kendall, C. G., 2008. Late Pleistocene to Holocene Sea Level Curve Derived from South Carolina Coastal Terraces: A Correlatable Datum for both 18O and Coral Reef Terrace Sea Level Curves, American Association of Petroleum Geologists/SEPM Joint Annual Meeting, San Antonio, Texas, Abstracts with Programs.

DePratter C. B. and J. D. Howard, 1981. Evidence for a Sea Level Lowstand Between 4500 and 2400 Hundred Years B.P. on the Southeast Coast of the United States. Journal of Sedimentary Petrology 51(4): 1287-1295.

DeVoe M. R. and F. J. Vernberg, 1992. Characterization of the Physical, Chemical and Biological Conditions and Trends in Three South Carolina Estuaries: 1970-1985 Winyah Bay and North Inlet Estuaries, v. 2. Charleston, S.C. Sea Grant Consortium: 1-115.

Gardner L. R. and D. E. Porter 2001. Stratigraphy and geologic history of a southeastern salt marsh basin, North Inlet, South Carolina, USA. Wetlands Ecology and Management 9: 371-385.

Gayes P.T., D.B. Scott, E.S. Collins and D.D. Nelson, 1992. A Late Holocene Sea Level Fluctuation in South Carolina. Quaternary Coasts of the United States: Marine and Lacustrine Systems, SEPM Special Publication 48: 155-160.

Montane, J.M. 2007. Geophysical and Stratigraphic Analysis of a southeastern Salt Marsh, North Inlet, SC. Dissertation Geological Sciences. Columbia, University of South Carolina: 124.

Neal A., 2004. Ground-Penetrating Radar and its use in Sedimentology; Principles, Problems and Progress. Earth Science Reviews 66 (3-4):261-330.

Topp G.C., J.L. Davis and A.P. Annan, 1980. Electromagnetic Determination of Soil Water Content: Measurements in Coaxial Transmission Lines. Water Resources Research, 16(3): 574-582.

Weaver Wendy, 2006. Ground Penetrating Radar Mapping in Clay: Success from South Carolina, USA. Archaeological Prospection 13: 147–150.

Wright E., A.C. Hine, S. L. Goodbred, and S.D. Locker, 2005. The Effect of Sea-level and Climate Change on the Development of a Mixed Siliciclastic-Carbonate, Deltaic 17 Coastline: Suwannee River, Florida, U.S.A. Journal of Sedimentary Research, 75: 621- 635.

SOUTHEASTERN GEOLOGY
V. 47, No.2, May 2010, p. 105-116

HYDROLOGY AND GEOLOGY OF A CREATED GROUNDWATER SLOPE WETLAND

STAN J. GALICKI

Department of Geology
Millsaps College
1701 N State St., Jackson, MS 39210
galics@millsaps.edu

JEANNIE R. B. BARLOW

USGS Water Science Center
308 S. Airport Road Jackson, MS 39208
jbarlow@usgs.gov

ABSTRACT

The origin and extent of a created slope wetland was investigated using hydrologic, geologic, and geomorphic methods. The area of investigation is situated on a gradual slope and supports hydrophytic vegetation such as black willow, soft rush, and cattail. The extent and elevation of the water table in the wetland was determined using a network of shallow piezometers. Head measurements at the source and within the wetland area documented the required saturation of the root zone in excess of 5% of the 235 ± 20 day growing season in central Mississippi. Based on several topographic surveys conducted over the past 51 years, the wetland's formation is a result of continued landscape alteration made since the late 1970s to accommodate Millsaps College's baseball field. Pleistocene age terrace deposits removed from the adjacent hill-top to level the playing surface were used in extending and re-contouring the adjacent slope which is composed of the Eocene age Yazoo Clay. Three 5 m auger holes drilled upslope of the source area of the wetland encountered well developed sand at the base of the terrace deposit. During construction, a swale in the Yazoo Clay on the slope was filled in with porous terrace material which created an unconfined aquifer on top of the impermeable Yazoo. Precipitation-sourced groundwater draining from the terrace sediment sources the wetland. Because the natural hydrology was only recently altered, only hydrophytic vegetation and a saturated root zone are required by the US Army Corp of Engineers to delineate the area as a wetland. Fully developed hydric soils have not had sufficient time to form. The created slope wetland encompasses approximately 0.5 hectare which is large enough to be protected under U.S. Army Corp of Engineers guidelines. The created slope wetland serves as an excellent educational research tool and highlights the important practical application of geology and hydrology in respect to engineering design and construction.

INTRODUCTION

Wetlands are typically thought of as topographically low areas surrounding, or adjacent to, coastal, lacustrine, and riparian ecosystems. Ground-water slope, or slope wetlands, are a unique class of wetland that form where a change in slope results in the unidirectional flow of water at or near the surface, which supports both hydrophytic vegetation and the conditions necessary to create hydric soils (Novitzki 1982, Brinson 1993, Smith et al. 1995). Slope wetland hydrology and biological resilience have been correlated with subsurface geology and hydrology of the bedrock. Stein et al., (2004) reported that southern California slope wetlands influenced primarily by regional groundwater flow from storage were more persistent and resilient than those sourced primarily by localized aquifers and precipitation. Shaffer et al. (1999), in a study of Portland, OR area wetlands, reported that slope wetlands

maintained the lowest water levels, extent, and duration of inundation as compared to other wetland types. Although typically small, natural slope wetlands are biologically diverse, can have important ecological implications in arid environments, and are increasingly coming under regulation (Stein et al. 2004). In urban settings, small created wetland gardens and parks are increasingly becoming a part of city landscapes as attractions and focal points. In addition to providing educational opportunities and aesthetic enjoyment, they are also habitat for endangered and critical species. (Chovanec 1994, Rosenberg 1996, Sun and Wang 2007).

This paper reports on the accidental creation of a slope wetland in the midst of a landscape dominated by century old red and post oaks on the Millsaps College campus in Jackson, Mississippi. The wetland formation has provided numerous opportunities for educational research, added ecologically and aesthetically to the campus landscape, and serves as an example of sustainable landscape management. Although, the formation of the wetland has had few negative consequences, campus planners have not always taken into account the terrace hydrology and this has contributed to the formation of a large and costly slope failure in the area.

Investigation of the study area was prompted by noticeably persistent high soil moisture conditions and the growth and development of plant species not typically encountered on the rolling upland topography of central Mississippi. High soil moisture areas were noted on campus, but the areas were maintained as grass lawn prior to 1998. In an initial study, Miles (1999) installed two piezometers130 m west-northwest of the study area to investigate the terrace aquifer response to precipitation as related to the development of a small slump that formed immediately following the 1998 slope alteration of the terrace area. In a second investigation, Hooks (2000) documented three species of hydrophytes: black willow (*Salix nigra*), southern cattail (*Typha latifolia*), and soft rush (*Juncus effusus*) within the study area. The objective of this study is to document wetland hydrology and its extent, the near subsurface

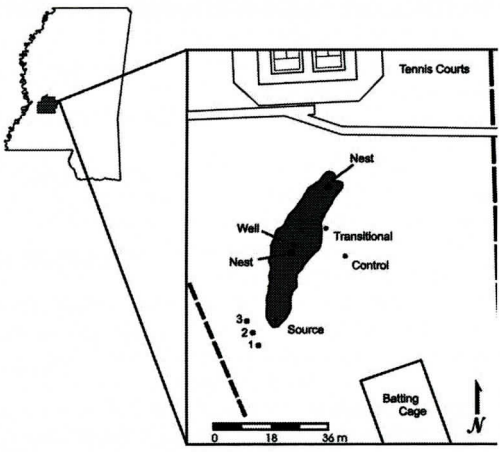

Figure 1. State of Mississippi with Hinds Co. and study area featuring the location of piezometers, nests, central well and auger holes.

geology, and demonstrate that landscape alteration of the local area created hydrology favorable for wetland development.

STUDY AREA

Millsaps College is an urban campus that encompasses approximately 297 ha (120 ac) located in northeastern Hinds County, Mississippi. The area of study is located adjacent to the baseball field on an eastward facing slope (Figure 1). Hinds County lies within the Jackson Prairies physiographic region, which consists of flat and rolling grasslands overlying deposits of limestone, marl and clays (Kelley 1974). Geologic units outcropping within the study area include the Eocene age Yazoo Clay Formation of the Jackson Group, which is overlain unconformably by approximately 6 m of Pleistocene age terrace deposits. The Yazoo Clay consists mainly of blue-green to blue-gray, fossiliferous clay which weathers yellow to yellowish brown. The terrace deposits contain gravels composed of chert and quartz with sands and some clay lenses. The terrace sands are red when weathered and the clays appear in a variety of colors, including red, yellow, pink, and purple (Moore et al. 1965).

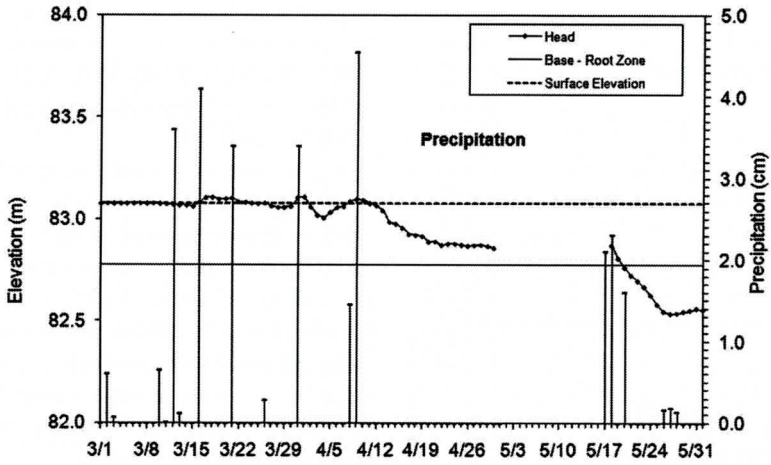

Figure 2. Water table elevation vs. time for the source piezometer. Vertical drop lines represent precipitation events.

METHODS

The origin and extent of the slope wetland was investigated using hydrologic, geologic, and geomorphic methods. Wetland hydrology was investigated using a network of piezometers, detailed geology through information obtained from several hand drilled auger holes, and landscape evolution over the past fifty-one years using historical topographic surveys of campus and a recent survey of the wetland.

The hydrology of the wetland was evaluated using a network of 5 cm diameter piezometers and a large 30.5 cm diameter well. During the spring of 2001, nine piezometers were installed in the wetland area (Figure 1). Three piezometers were individual installations and the other six were installed in two nests composed of three piezometers each. The nests were installed in the center of the wetland area and also near the down slope terminus of the wetland. Piezometers were constructed of slotted and solid polyvinyl chloride (PVC) pipe fitted with bases and vented caps. A post-hole digger was used to bore 15 cm diameter holes in which to install the piezometers. After piezometer installation, sand was packed around the slotted intervals and the remainder of the annulus filled with granular bentonite clay. The piezometers within the nests were installed at the apices of a triangle, 30 cm apart. The slotted intervals for each of the three piezometers within each nest were at depths from 38-48 cm, 53-63 cm, and 65-75 cm to examine for the potential of vertical flow gradients from beneath the root zone. The remaining piezometer installations were similar and consisted of a control piezometer slotted to a depth of 80 cm outside the apparent wetland area, a 61 cm piezometer near the apparent upslope source, and a 61 cm piezometer which is located on the east side of the wetland in an area that appeared to be transitional between the wetland and surrounding terrain. A 1 meter deep well consisting of 30 cm diameter slotted PVC was installed in the center of the wetland area. The large diameter well was originally designed to accommodate the float for a Stevens Chart Recorder; the recorder was not reliable and was never utilized. Water level measurements made during the 2002 growing season were done using meter stick fitted with an electronic sensor. Campus precipitation data from January 2002 to October 2002 was obtained from records kept by the buildings and grounds department.

Geology of the source area was investigated by analyzing samples taken during the drilling of three 5 cm diameter auger holes. Auger holes were drilled to a depth of 5 m into the Pre-loess Terrace deposits immediately upslope from the head of the wetland (Figure 1). A composite sample consisting of sediment retrieved each 30

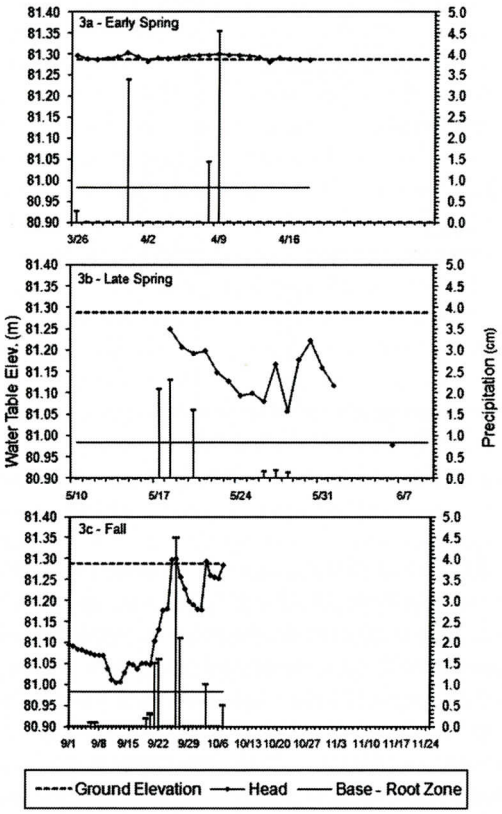

Figure 3a, b, and c. Water table elevation vs. time for the central well. Vertical drop lines represent precipitation events.

cm during drilling was collected in plastic bags for transport to the lab. Samples were dried in a laboratory oven at 100° C until no further loss in weight was detected. The percentage of sand and gravel versus silt and clay was determined on each sample by wet sieving approximately 100 g through a US 230 mesh (63 μm) sieve. The portion of the sample retained on the sieve was washed into an aluminum dish and dried. The percentage of sand and greater size particles was calculated relative to the initial sample weight prior to sieving.

Soils from the wetland area were assessed by extracting a 56 cm soil core located between the source and control piezometers. Once extracted, the core was immediately bisected and photographed. Soil color determinations of each horizon were made using Munsell soil color charts to document the soil conditions in their original state before any drying occurred. Indicators of hydric soils were assessed using the U.S. Department of Agriculture (USDA) Natural Resources Conservation Service criteria (USDA/NRCS 2003).

Maps from historical topographic surveys obtained from the Millsaps College Physical Plant were used to document changes in topography through time. Campus topographic surveys done in 1958, 1985, and 1997 were normalized to a uniform scale and referenced using the James Observatory as a landmark. A topographic survey using a Sokkia SET 600 Total Stations transit was made to create a recent topographic map of the area.

RESULTS

For several weeks prior to monitoring water levels in the wetland, and periodically during the course of the study, the piezometer nests were evaluated for indications of a vertical hydraulic gradient. Neither the nest placed in the center of the wetland nor the nest installed at the down slope terminus indicated a vertical component of groundwater flow.

The hydrograph for the source piezometer, shown in Figure 2, indicates that the soil was saturated within 30 cm of the surface for a nine week period beginning on March 1st. The water level was maintained at ground level throughout March and most of April. The lack of precipitation in late April and May resulted in the decrease in the water level by June, and an eventual drop below the 30 cm horizon. Fall measurements were not made. Water level in the well was at, or within, 30 cm of the surface for three consecutive weeks in late March and April, two weeks in late May and early June, and five weeks in September and early October (Figure 3a, b, and c). The water table was within the root zone for 100% of the measurement days.

Water levels in the transitional piezometer only sporadically reached the root zone for several days during or following heavy precipitation in the late winter and early spring, summer, and fall (Figure 4a, b, and c). The consistent readings in June were due to water trapped by

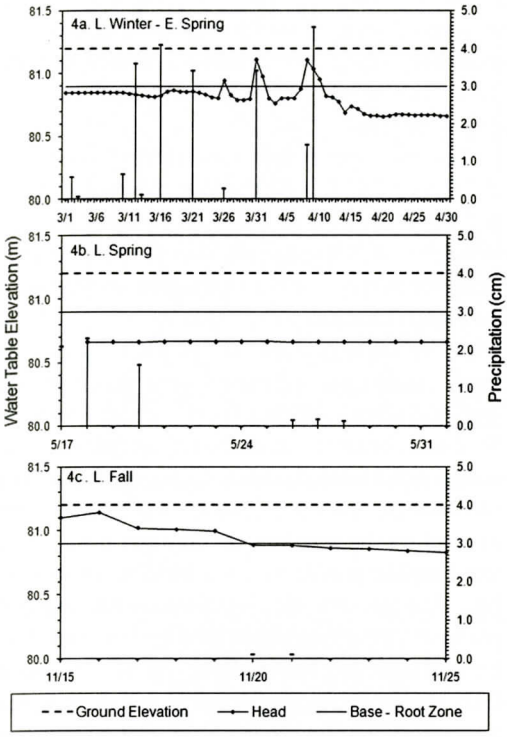

Figure 4a, b, and c. Water table elevation vs. time for Transitional Piezometer Vertical drop lines represent precipitation events. Note that no precipitation data was available for the fall sampling.

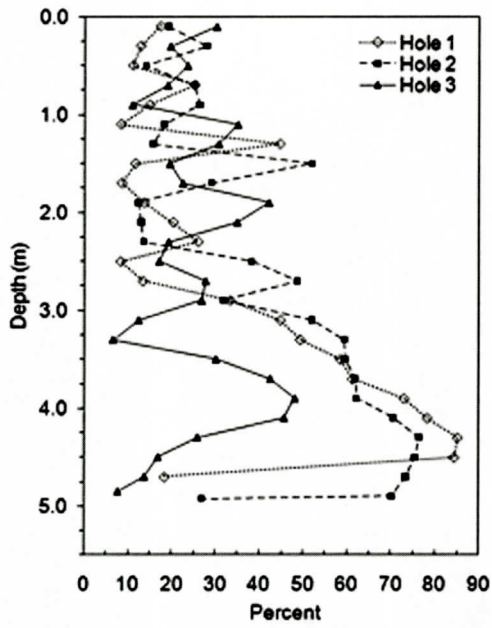

Figure 5. Percent sand and gravel versus depth for auger holes 1, 2, and 3.

the base of the piezometer. Although the actual depth to the water table during this period is not known, but it is not within the root zone. The control piezometer only recorded water within the root zone for two of the first 24 days of measurement in apparent response to storm events. The piezometer was destroyed by grounds keeping crews and was not replaced.

The results of the percent sand and gravel analysis done on 75 samples taken from auger holes 1, 2, and 3 are displayed Figure 5. In all three holes artificial fill material, indicated by mortar, charcoal, and ceramic material was encountered at approximately 2.0 to 2.4 m. Samples from auger holes 1 and 2 indicate a zone of well developed sand occurring approximately 4.0 to 4.9 m in depth. The zone is characterized by an increase in sand percentages above 60%. The sand consists of coarse to very coarse grained quartz and chert sand with pebbles, granules and cobbles. Cobble sized grains ranging up to 2 cm in were encountered in the lower portion of the sand zone within both holes, but were much more abundant in auger hole 2. The sand in auger hole 3 is not as well developed (maximum sand and gravel percentage of 48%) as in auger holes 1 and 2 to the south. The top of the Yazoo Clay in all three auger holes was identified at approximately 4.9 m as yellow to yellow brown clay.

The upper 30 cm of the soil core consisted of approximately 6 cm of organic horizon at the surface which transitioned into silty clay between 6 and 11 cm (Figure 6). The remaining 17-30 cm appeared to be composed of fill material ranging in size from clay to gravel. The Munsell colors ranged from 2.5 YR 2/5 to 2.5 YR 4/4. A distinct clay interval (Munsell value of 7.5 YR 5/8) was present at approximately 30-40 cm depth; this layer transitioned into sandy clay (Munsell value of 7.5 YR 4/6) at 40-56 cm. The basal interval is characteristic of terrace sediment. A strong hydrogen sulfide odor was detected at the bottom of the core. It is worth noting that two approximately 5 cm diameter

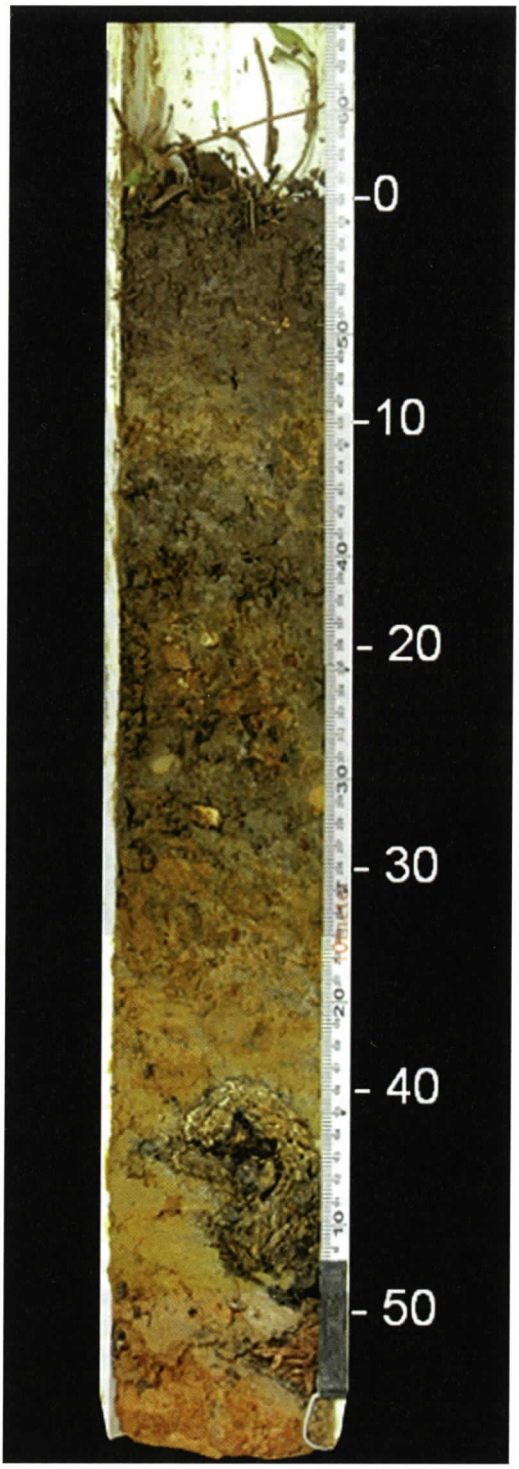

pieces of decaying woody debris were found between depths of 40-56 cm. Also, almost immediately after the core was extracted, the hole filled with water to a level above the 30 cm required interval.

Campus topographic surveys made in 1958, 1985, and 1997 indicate that the topography within the study area has been considerably altered. Figure 7 displays the recent and 1958 topographic surveys of the study area. Preliminary landscape changes were made in the late 1970s with the construction of the men's baseball field. Additional changes were made in the late1990s with further work on the baseball field and construction of the tennis courts to the north of the wetland area. Cross section A-A', constructed near the axis of the wetland, (Figure 8) displays the relationship between the current topographic profile and the historic 1958 profile. The present slope maintains an average grade of 12% along the axis of the wetland. The terrace sand interval and the top of the Yazoo Clay shown on the profile are based on samples taken from the three auger holes drilled near the top of the terrace.

DISCUSSION

Wetland determination as defined by the U.S. Army Corp of Engineers (USACE) requires the documentation of three parameters: the presence of hydrophytes, development of hydric soils, and saturated soil conditions in the root zone for a portion of the growing season. In areas unaffected by anthropogenic activities each of the three conditions must be documented. However, in situations where anthropogenic activities have caused the formation of the wetland, positive indicators are only required for two of the three parameters cited. The alterations that have taken place in the study area have created a condition defined by the USACE

Figure 6. Photograph of wetland core. Depths from surface are indicated to the right of the core are in cm.

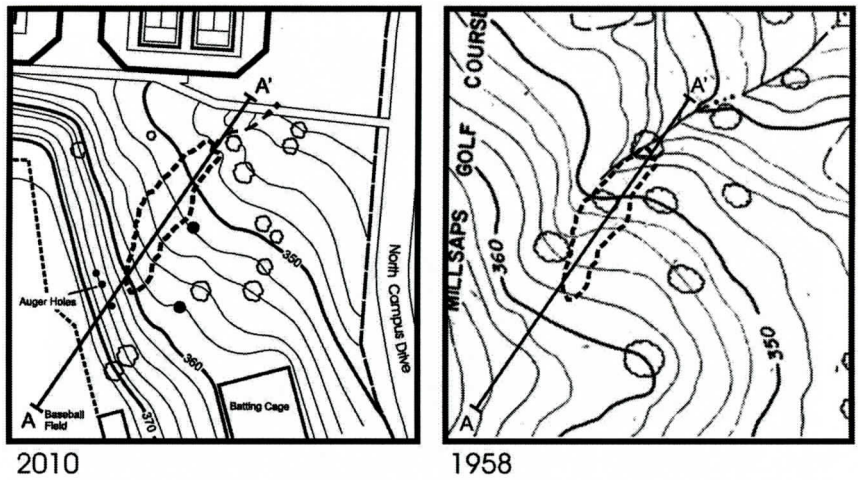

Figure 7. Topographic maps of the slope wetland area in 2010 and 1958.

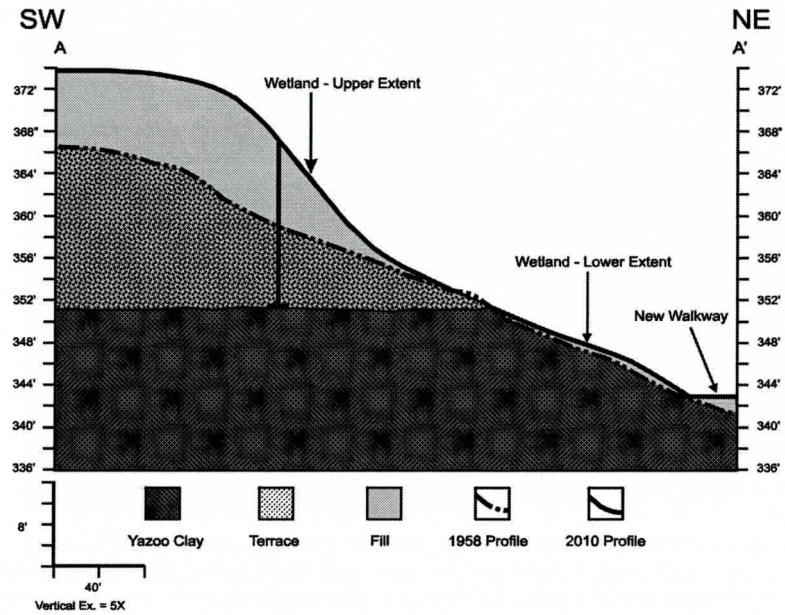

Figure 8. Cross section A-A' through the axis of the wetland with position of auger holes and wetland limits indicated.

as a man-induced or created wetland, which is defined as an area that has developed at least some characteristics of naturally occurring wetlands due to either intentional or incidental human activity and are not sustained solely by irrigation practices (USACE 1987, p. 82; Wakeley 1994). Created wetlands are primarily delineated by wetland hydrology and presence of hydrophytes because hydric soils, common in natural wetlands, may take time to develop and therefore, may not be present in more recently created wetlands.

The study area can be easily distinguished by the hydrophytic vegetation that thrives within its boundaries. Hooks (2000) identified three key hydrophytes within the area which include the black willow (*Salix nigra*), southern cattail (*Typha latifolia*), and soft rush (*Juncus effusus*);

Figure 9. Wetland photograph taken facing southwest in the winter of 2001. Black willows near center of wetland area had become well established. Recommendation to cease traditional landscaping was made just after this photo was taken.

Figure 10. Wetland photograph taken facing south in the late spring of 2002. Within the heart of the wetland marsh grass and cattails had become well established. Source area can be seen to the extreme right-hand side of photo. The wetland was accidentally mowed several weeks before this photo was taken, no trees were removed.

all three species are classified as obligate wetland plants (USACE 1987). The bristly buttercup (*Ranunculus hispidus*) which is well adapted for moist soils and crawfish (*Procambarus sp.*) burrows have also been identified. The zone of isolated hydrophytes on the slope is surrounded by large, well established red and post oaks (*Quercus rubra* and *Quercus stellata*) which are mesophytes and grow in conditions that are not extremely wet or dry. They are not normally found in wetland habitats but can survive in wet conditions (USDA/NRCS 2009).

The water table requirement is derived from the USACE Wetland Delineation Manual, which requires the saturation of the root zone to a depth of approximately 30.5 cm (12 in) below the surface for at least 5% of the growing season (USACE 1987). The length of the growing season is defined as the number of frost free days. Based on a 108 yr record the average and stan-

Figure 11. Wetland photograph taken facing northwest towards the source in 2004. Second stand of black willow had become established at the source since mowing in 2002.

dard deviation of frost free days in Jackson, Mississippi is 235± 20. The average growing season extends from March 19th to Nov. 7th (NWS 2005). Five percent of the growing season in Jackson, MS, as required by USACE, would be 12 days. The water levels in both the source piezometer and the central were within 30 cm of the surface for well over 12 days during the growing season as required by the USACE guidelines. Wetlands are generally at their optimum extent during the spring (USACE 1987). In early spring, water levels in the transitional piezometer maintained saturation just beneath the 30 cm zone for a five week interval, suggesting that it was truly near the margin of the wetland. The transitional piezometer did not saturate within 30 cm of the surface again until late fall; the sampling was not adequate to document a two week period. The results of water table measurement clearly indicate saturated conditions in the root zone for the required period during the growing season in the vicinity of the central well and source piezometers, and outwards towards the transitional piezometer.

The core analysis revealed that conditions are present for the development of hydric soils within the wetland area. The main indicator was a strong hydrogen sulfide odor occurring in the bottom 40-56 cm interval which was likely due to the presence of decaying woody debris. Saturation of the root zone, one of the primary requirements for hydric soil formation, was also observed at the core location. If the wetland area continues to experience sustained periods of inundation, the further development of hydric soils within the area is expected.

There is no documentation of wetlands on campus prior to 1998. Further analysis of Miles (2000) data indicates a relationship between the recharge of the terrace aquifer and precipitation. The change in head in two piezometers immediately following storm events $\geq$ 2.0 cm over a six month period in 1998 has a correlation coefficient of 0.67 (n=9). The terrace aquifer sources the area studied by Miles and also the area studied here. By the spring of 2001, a recommendation was made to stop mowing the area when immature black willows were observed and the grass had become difficult to maintain using standard landscaping techniques due to the saturated soils (Figure 9). By the spring of 2002 the young willows had already reached a height of 4.5 m and other obligate plants had become established (Figure 10).

On the 1958 topographic survey, a distinct

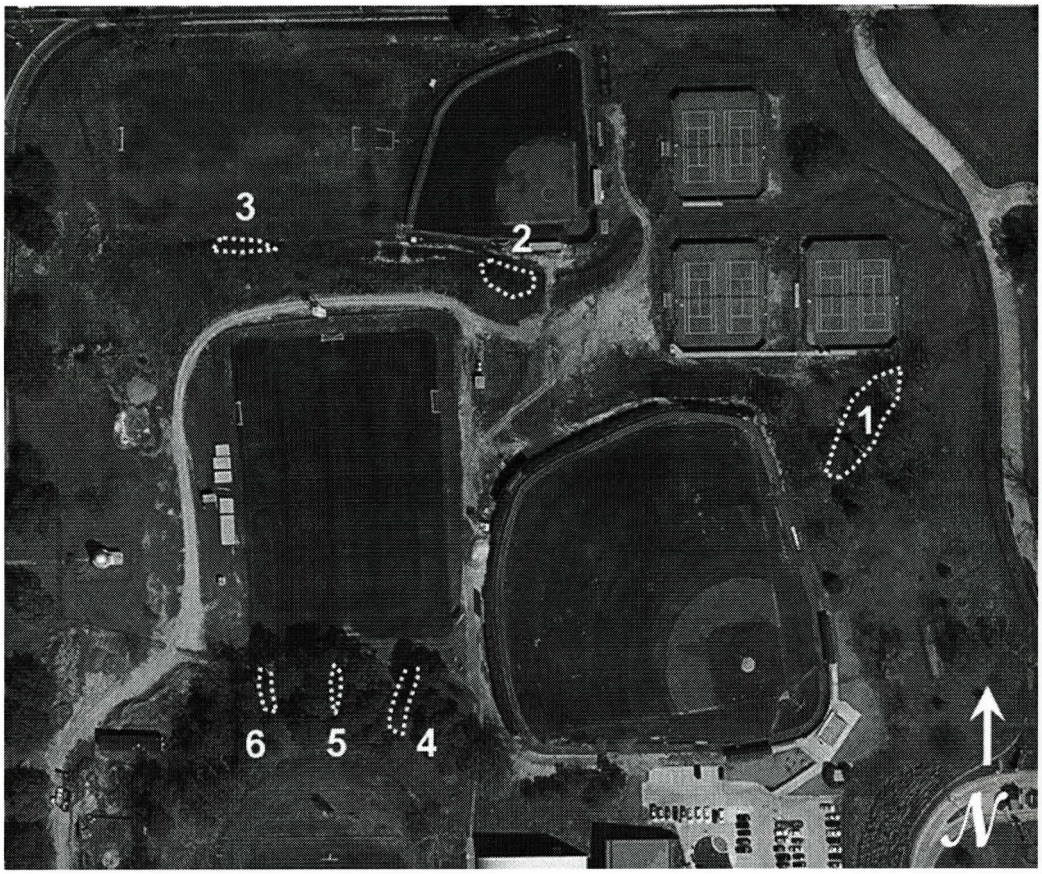

Figure 12. Active seeps in the north campus area in a 2002 aerial photo. 1) Slope wetland reported in this paper; 2) slope failure area with black willow reported on by Miles (1999); 3) additional area investigated by Miles (1999), also populated by young black willow; 4 and 5) active seeps on south facing slope. Note, the zone across the north slope which included both areas 2 and 3 was re-worked in the summer of 2007; a 100 m long by 2.3 m high precast block retaining wall was constructed. In the winter of 2007 the slope failed and displaced the wall over 3.0 m horizontally to the north.

swale is indicated which closely corresponds to the outline of the present wetland. The leveling of the 4 ha (10 ac) area immediately to the west of the wetland to accommodate the baseball field and an additional practice field resulted in the removal and redistribution of up to 5 m of terrace sediment. As shown in Figures 7 and 8, the surplus material was used as fill to extend the level of the playing surface to the east. The swale developed in the Yazoo Clay may have been part of relict drainage system off the hill to the west. It is probable that other similar drainages cut into the Yazoo Clay served as outlets for eroding terrace sediments and became filled in with sand as the terrace sand was deposited. The contact between the terrace deposit and the Yazoo Clay is at an elevation of approximately 106.9 m (351 ft) msl. As the slope was re-contoured in 1997, the swale was filled in with a mixture of porous sands and clay from the overlying terrace. The location of the terrace sand which developed on top of the Yazoo Clay facilitates the delivery of groundwater to the wetland. By 2004 a second stand of willows had become established near the source area (Figure 11). The 4 ha area leveled for the ball fields is isolated from groundwater flow laterally due to its elevation, and from below by the underlying

Yazoo Clay which serves as a regional aquiclude. Although a small percentage of water in the aquifer may be derived from irrigation of the playing fields, the combined topography, geology, and correlation between precipitation and head change indicates that the primary source of ground water to this area is via precipitation that infiltrates through the terrace sediment.

Various hydrologic indicators were used to estimate the extent of the slope wetland. Determining the source and terminus of the wetland area was relatively easy. The head of the wetland was indicated by vegetation and the boundary between firm and saturated soil towards the head of the slope. The terminus formed as water left the wetland area as the graded terrace deposits feathered out and water seeped out and drained on the surface. Assuming the wetland is symmetrical, the maximum width was estimated to equal twice the distance between the central well and the transitional piezometer (Figure 1). The approximate area of the slope wetland is 447 m^2 (~0.5 Ha or 4809 ft^2).

The wetland area studied here is not the only hydrologically active area associated with the terrace deposits and affected by landscape alterations (Figure 12). Miles (1999) attributed slope failure on the north facing slope (area 2), 130 m northwest of the wetland area, to high water saturation in the terrace deposits on the recently re-contoured slope. Campus planners and construction engineers failed to note the significance and connection between the "wet area" noted on the 1997 survey which became the wetland, the small slump that formed in 1998, and the hydrologic properties of the terrace sediment. Galicki (2009) reported on a major slope failure which encompassed the zone between areas 2 and 3 on Figure 12. A 100 m by 2.3 m high pre-cast concrete block retaining wall was built along the full extent of the northern slope in the summer of 2007. Over-steepening of the slope, improper back-fill material, and poor drainage behind the wall resulted in a 100 m long failure of the slope with a maximum vertical and horizontal displacement of 2 m and 3 m respectively. The hydrologic properties of terrace deposits again played an important role in the alteration of the campus landscape, except this time, it was large and costly. The design of the second wall provided for adequate drainage from the terrace deposits to prevent future failure. Areas 4, 5, and 6 on the south slope are also hydrologically active in the north campus area; neither is as large as the slope wetland reported here. These hydrologically active areas serve as excellent educational research tools but also highlight the important practical application of geology and hydrology in respect to engineering design and construction.

CONCLUSIONS

Wetland hydrology, vegetation, and developing soils were documented on a slope following landscape modification. The presence of hydrophytic vegetation and the documentation of saturated conditions in the root zone for more than two weeks of the growing season permit classification of the study area as a created wetland. Hydric soils appeared to be developing as noted by a strong sulfur odor, and decaying woody debris within a soil core taken from the wetland area. The slope wetland formation is a result of landscape modification and the infilling of a former drainage feature in the Yazoo Clay with permeable terrace material. Wetland hydrology is maintained by the movement of groundwater from the overlying terrace deposit through sand developed at the base of the Pleistocene terrace near the head of the wetland.

ACKNOWLEDGEMENTS

We would like to thank the Gulf Coast Association of Geological Societies for partially funding this research through an undergraduate student research grant.

REFERENCES CITED

Brinson, M. 1993, A hydrogeomorphic classification of wetlands: Technical Report WRP-DE-4, U.S. Army Corp of Engineers Waterways Experiment Station, Vicksburg, MS.

Chovanec, A., 1994, Man-made wetlands in urban recreational areas-a habitat for endangered species?: Land-

scape and Urban Planning, v. 29, p. 43-54.
Galicki, S.J. 2009, Slope failure at Millsaps College, Jackson, Mississippi: Mississippi Academy of Science Abstracts Issue 54:61, Olive Branch, MS.
Hooks, S., 2000, Wetland delineation on Millsaps Campus: Directed Study, Millsaps College, Jackson, MS.
Kelley, A. 1974, Topography. In: Cross, R.D. ed. Atlas of Mississippi. Jackson: University Press of Mississippi, 4 p.
Miles, J., 1999, A hydrological and geophysical study of an unconfined aquifer at Millsaps College: Millsaps College Honors Program, Jackson, MS.
Moore, W.H., Bicker, A.R., McCutcheon, T.E., and Parks, W.S., 1965, Hinds County geology and mineral resources: Bull. MS Geological Economic and Topographical Survey, No. 105, p. 41-49, Jackson, MS.
National Resources Conservation Service, 1997, National Water and Climate Center: Climate analysis for wetlands by county: ftp.wcc.nrcs.usda.gov/support/climate/wetlands/ms /28049.txt.
National Weather Service, 2005, Frost data (dates and growing season days) at Jackson, MS
from 1896 current through 2004: www.srh.noaa.gov/jan/frostfreq.html.
Novitzki, R.P., 1982, Hydrology of Wisconsin wetlands: Geological and Natural History Survey Resources Program, Madison, WS.
Rosenberg, E., 1996, Public works and public space: rethinking the urban park, Journal of Architectural Education, v.50, p. 89-103.
Shaffer, P.W., Kentula, M.E., and Gwin, S.E., 1999, Characterization of wetland hydrology using hydrogeomorphic classification: Wetlands, v. 19, p. 490-504.
Smith, R.D., Ammann, A., Bartoldus, C., and Brinson, M.M., 1995, An approach for assessing wetland functions using a hydrogeomorphic classification, reference wetlands, and functional indices: Wetlands Research Program Technical Report WRP-DE-9, U.S. Army Corp of Engineers, 16 p.
Stein, E.D., Mattson, A., Fetscher, A.E., and Halama, K.J., 2004, Influence of geologic setting on slope wetland hydrodynamics: Wetlands, v. 24, p. 244-260.
Sun, G.Y., and Wang H.X. 2007, Garden wetland: a new type of constructed wetland: Wetland Science, v. 5, p. 7-12.
USDA/NRCS, 2009, Plants Database: http://plants.usda.gov/index.html.
USDA/NRCS, 2003, Field Indicators of Hydric Soils in the United States, Version 5.01. G.W. Hurt, P.M. Whited, and R.F. Pringle (eds.). USDA, NRCS in cooperation with the National Technical Committee for Hydric Soils, Fort Worth, TX.
U.S. Army Corps of Engineers, 1987, Corps of Engineers wetlands delineation manual: U.S. Army Corps of Engineers Technical Report Y-87-1, 82 p.
Wakeley, J.S. 1994, Identification of wetlands in the southern Appalachian region and the certification of wetland delineators: Water, Air, and Soil Pollution, v. 77, p. 217-226.